![University of York]

![White Rose university consortium — Universities of Leeds, Sheffield & York]

eprints@whiterose.ac.uk
https://eprints.whiterose.ac.uk/

1 **Chemically-defined cytokine-free human hematopoietic stem cell expansion**

2

3 **Authors:**

4 Masatoshi Sakurai[1,2*], Kantaro Ishitsuka[3*], Ryoji Ito[4], Adam C Wilkinson[1,5,6], Takaharu

5 Kimura[3], Eiji Mizutani[3,7], Hidekazu Nishikii[8], Kazuhiro Sudo[9], Hans Jiro Becker[1,3],

6 Hiroshi Takemoto[10], Tsubasa Sano[11], Keisuke Kataoka[2,12], Satoshi Takahashi[13], Yukio

7 Nakamura[9], David G Kent[14,15], Atsushi Iwama[16], Shigeru Chiba[8], Shinichiro Okamoto[2],

8 Hiromitsu Nakauchi[6,7,17], and Satoshi Yamazaki[1,3,17]

9

10 **Affiliations:**

11 [1]Division of Stem Cell Biology, Center for Stem Cell Biology and Regenerative

12 Medicine, The Institute of Medical Science, The University of Tokyo, Japan

13 [2]Division of Hematology, Department of Medicine, Keio University School of Medicine,

14 Tokyo, Japan

15 [3]Laboratory of Stem Cell Therapy, Faculty of Medicine, University of Tsukuba, Ibaraki,

16 Japan

17 [4]Human Disease Model Laboratory, Central Institute for Experimental Animals,

18 Kawasaki, Kanagawa, Japan

19 [5]MRC Weatherall Institute of Molecular Medicine, University of Oxford, Oxford, UK

20 [6]Institute for Stem Cell Biology and Regenerative Medicine, Department of Genetics,

21 Stanford University School of Medicine, Lorry I. Lokey Stem Cell Research Building,

22 265 Campus Drive, Stanford, CA, USA

23 [7]Division of Stem Cell Therapy, Distinguished Professor Unit, The Institute of Medical

24 Science, The University of Tokyo, Tokyo, Japan

25 [8]Department of Hematology, Faculty of Medicine, University of Tsukuba, Ibaraki, Japan.

26 [9]Cell Engineering Division, RIKEN BioResource Research Center, Tsukuba, Japan.

27 [10]Department of Neuroscience, Drug Discovery & Disease Research Laboratory,

28 Shionogi; Business-Academia Collaborative Laboratory (Shionogi), Graduate School of

29 Pharmaceutical Sciences, The University of Tokyo, Japan

30 [11]Pharma Solutions, Nutrition & Health, BASF Japan Ltd., Tokyo, Japan

31 [12]Division of Molecular Oncology, National Cancer Center Research Institute, Tokyo,

32 Japan

33   [13]Division of Clinical Precision Research Platform, The Institute of Medical Science,

34   The University of Tokyo, Tokyo, Japan

35   [14]Department of Biology, York Biomedical Research Institute, University of

36   York, York, UK

37   [15]Wellcome MRC Cambridge Stem Cell Institute, University of Cambridge,

38   Cambridge, UK

39   [16]Division of Stem Cell and Molecular Medicine, Center for Stem Cell Biology and

40   Regenerative Medicine, The Institute of Medical Science, The University of Tokyo, Japan

41   [17]Corresponding authors. Email: y-sato4@md.tsukuba.ac.jp (S.Y.);

42   nakauchi@stanford.edu (H.N.)

43   *These authors contributed equally.

44

Abstract:

Hematopoietic stem cells (HSCs) are a rare cell type that reconstitute the entire blood and immune systems following transplantation, a curative cell therapy for a variety of hematological diseases[1,2]. However, the low number of HSCs makes both biological analyses and clinical application difficult, and the limited ability to expand human HSCs ex vivo remains a substantial barrier to the wider and safer therapeutic use of HSCT[3]. While various reagents have been tested in attempts to stimulate human HSC expansion, cytokines have long been thought to be essential for supporting HSCs ex vivo[4]. Here we report the establishment of a novel culture system that supports the long-term ex vivo expansion of human HSCs, achieved through the complete replacement of exogenous cytokines and albumin with chemical agonists and a caprolactam-based polymer. A phosphoinositide 3-kinase activator, in combination with a thrombopoietin-receptor agonist and the pyrimidoindole derivative UM171 were sufficient to stimulate expansion of umbilical cord blood HSCs capable of serial engraftment in xenotransplantation assays. Ex vivo HSC expansion was further supported by split-clone transplantation assays and single cell RNA-sequencing analysis. We envision that this chemically-defined expansion culture system will help to advance clinical HSC therapies.

Main text:

Self-renewing multipotent hematopoietic stem cells (HSCs) are a rare bone marrow (BM) cell population that support life-long hematopoiesis[5-8] and hematopoietic system reconstitution following HSC transplantation (HSCT) [1]. HSCs can also be collected from umbilical cord blood (CB), which represents a highly-accessible source for transplantation but often contain too few HSCs for successful engraftment and durable hematopoietic reconstitution. Ex vivo expansion of human HSCs, particularly CB-derived HSCs, is therefore a major goal in hematology and one that remains a substantial barrier to the wider and safer therapeutic use of HSCs[3].

Various recombinant cytokines are commonly added to human HSC cultures in attempts to promote HSC expansion, usually in combination with serum albumin[4]. These cultures generally support short-term maintenance of HSCs but fail to expand functional HSCs. However, two-week ex vivo expansion of human HSCs has been achieved by the addition of small molecules, StemRegenin 1 (SR-1)[9] and UM171[10]. Clinical trials using these approaches to expand CB HSCs prior to transplantation have reported encouraging results[2,11]. Other recent approaches have included use of 3-dimensional zwitterionic hydrogels[12], addition of novel growth factors[13], or combinations of small molecule inhibitors[14]. These methods have highlighted the importance of collaboration between chemical biology and stem cell biology to overcome this major barrier in hematology.

A chemically-defined cytokine-free media

Working towards the goal of expanding HSCs ex vivo, we recently established a long-term ex vivo expansion system for functional mouse HSCs by optimizing the concentrations of recombinant stem cell factor (SCF) and thrombopoietin (THPO), and replacing serum albumin for the synthetic polymer polyvinyl alcohol (PVA) [15,16]. Use of PVA avoided the batch-to-batch variability associated with serum albumin[17] and culture contamination with albumin-associated impurities that promote HSC differentiation. While mouse HSCs expanded rapidly in these conditions, human HSC expansion was more limited. When we compared the proliferation of mouse BM $Kit^+Sca-1^+Linage^-$ (KSL) HSPCs with human CB $CD34^+CD38^-$ HSPCs in PVA-based media supplemented with SCF and THPO[15], mouse HSPCs proliferated ~18-fold in 7 days while human

97   HSPCs only proliferated ~3-4-fold during the same time (**Figure 1a**). To examine the

98   difference between mouse and human HSPCs during these cultures, we analyzed the

99   phosphorylation status of major signaling pathways (PI3K, JAK/STAT, MAPK) linked

100   to SCF and THPO signaling[8,18,19]. Significant decreases in PI3K and AKT were observed

101   in human cells (**Figure 1b**, **Extended Data Figure 1a, b**). The PI3K phosphorylation

102   signal was also significantly decreased in human CD34$^+$CD38$^-$CD90$^+$CD45RA$^-$CD49f$^+$

103   phenotypic HSCs (**Extended Data Figure 1c**).

104   Based on these results, we hypothesized that we could improve human HSPC

105   expansion by activating PI3K-AKT signaling. We therefore evaluated chemical agonists

106   740Y-P (a PI3K activator) and SC79 (an AKT activator) in human HSPC cultures. While

107   SC79 did not improve expansion efficacy, 740Y-P significantly increased the number of

108   CD34$^+$ cells (**Figure 1c**) and CD34$^+$CD45RA$^-$ cells in 7-day cultures (**Extended Data**

109   **Figure 1d**). Furthermore, addition of 740Y-P significantly increased PI3K

110   phosphorylation in CD34$^+$CD38$^-$CD90$^+$CD45RA$^-$CD49f$^+$ cells (**Extended Data Figure**

111   **1e**). These results suggested that chemical activation of the PI3K pathway was sufficient

112   to improve human HSPC proliferation.

113   Previous studies have shown that SCF stimulates HSC cell cycle entry via the

114   PI3K/AKT/FOXO pathway[20-23]. We therefore hypothesized that we could replace SCF

115   with 740Y-P in human CD34$^+$ HSPCs cultures. No significant differences were observed

116   in the 7-day cell proliferation in THPO and 740Y-P with or without SCF (**Figure 1d**),

117   suggesting that SCF can be replaced with a PI3K activator. Cell cycle analysis confirmed

118   that the frequency of S/G2/M cells was comparable (**Extended Data Figure 1f**) while

119   colony forming unit (CFU) assays showed similar increases in multipotent granulocyte-

120   erythrocyte-monocyte-megakaryocyte (GEmM) CFUs in the presence or absence of SCF

121   (**Extended Data Figure 1g**). These results suggested that SCF was replaceable with

122   740Y-P in ex vivo human HSPC cultures.

123   We previously reported that recombinant proteins could destabilize HSC

124   cultures[15]. Recently, we found that chemical THPO receptor agonists (THPO-RAs) could

125   be used to induce human HSC expansion[24]. We therefore examined whether we could

126   replace recombinant THPO with THPO-RAs in PVA-based media containing 740Y-P.

127   Initial screening for optimal THPO-RAs was performed using a THPO-dependent MPL-

128   expressing cell line reported to proliferate in THPO-supplemented PVA conditions[25]. Of

129   the three THPO-RAs tested, only butyzamide supported cell proliferation (**Extended**

130   **Data Figure 1h**). We validated that butyzamide stimulated human CD34^{+} cell

131   proliferation in PVA-based media containing 740Y-P (**Extended Data Figure 1i**).

132   Surprisingly, when compared to the THPO and 740Y-P cultures, the butyzamide and

133   740Y-P cultures displayed significantly improved 7-day proliferation (total, CD34^{+} and

134   CD34^{+}CD41^{-}CD90^{+}CD45RA^{-} cell numbers) and GEmM CFU numbers (**Figure 1e,**

135   **Extended Data Figure 1j, k**). However, there was no additive effect of THPO and

136   butyzamide (**Extended Data Figure 1j**). In summary, these results confirmed that human

137   CD34^{+} HSPCs could be grown without exogenous cytokines by replacing SCF and THPO

138   with 740Y-P and butyzamide, respectively.

139   We next titrated 740Y-P and butyzamide concentrations for CD34^{+} cell

140   expansion and identified the combination of 1 µM 740Y-P and 0.1 µM butyzamide as

141   optimal for cell expansion, in terms of both total and CD34^{+} cell expansion (**Figure 1f**).

142   We defined this combination of 740Y-P (1 µM) and butyzamide (0.1 µM) as two

143   activators (2a) media. Using this media composition, we next examined long-term

144   stability of CD34^{+} cell cultures. Although total cell numbers increased during 14-day

145   cultures, the number of phenotypic CD34^{+} cells decreased between day 7 and 14, and the

146   cultures became dominated by CD41^{+} cells (**Figure 1g**, **Extended Data Figure 1l**).

147   Consistent with accumulation of these CD41^{+} megakaryocyte-lineage cells (**Extended**

148   **Data Figure 1m**), significant increases in megakaryocyte (MgK) CFUs were observed in

149   the day 14 cultures (**Extended Data Figure 1n**). Additionally, while 1×10^4 cells from 7-

150   day 2a cultures engrafted robustly in immunodeficient NOD/Shi-scid IL-2Rγ[null] (NOG)

151   mice[26], chimerism was not detected from 14-day 2a cultures (**Extended Data Figure 1o,**

152   **p**). Together, these results suggested that although 2a cytokine-free media supported

153   human HSCs short-term, it was not sufficient to stabilize longer-term expansion.

154

155   ***Long-term ex vivo HSC cultures***

156   Based on our 2a culture results, we searched for potential MgK inhibitors to

157   stabilize long-term ex vivo HSC expansion. We evaluated two reported HSPC expansion

158   compounds, SR-1[9] and UM171[10]. Addition of UM171 increased the total, CD34^{+} and

159   CD34$^+$EPCR$^+$ cell numbers after 7-days (**Figure 2a, Extended Data Figure 2a**). In 14-

160   day UM171 supplemented cultures, total, CD34$^+$, CD34$^+$EPCR$^+$ and

161   CD34$^+$EPCR$^+$CD90$^+$CD45RA$^-$ITGA3$^+$ cells were significantly increased while CD41$^+$

162   cell numbers were reduced (**Figure 2b, Extended Data Figure 2b**). Furthermore, the

163   expansion of CD34$^+$EPCR$^+$CD90$^+$CD45RA$^-$ITGA3$^+$ cells was significantly higher with

164   UM171 at 70 nM as compared to than 35 nM (**Extended Data Figure 2c**). Meanwhile,

165   the addition of SR-1 induced apoptosis (**Extended Data Figure 2d**). This three activator

166   (3a) media cocktail of UM171 (70 nM), 740Y-P (1 µM) and butyzamide (0.1 µM)

167   continued to stimulate proliferation over a 30-day culture by ~14-fold (**Figure 2c**). These

168   results suggested that HSPCs may be stably expanding in the 3a media.

169   To evaluate the in vivo engraftment and differentiation potential of the cultured

170   HSPCs, we performed xenotransplantation assay. We transplanted 1x10^4 CD34$^+$ cells

171   before culture (fresh) and after 10-day or 30-day cultures. Significantly higher human

172   CD45$^+$ PB chimerism was observed in the 10-day and 30-day culture groups, with

173   chimerism increasing over time (**Figure 2d, Extended Data Figure 2e**). BM analysis at

174   16- and 24-weeks also identified significantly higher human cell chimerism in the

175   cultured HSPC groups (**Figure 2e, Extended Data Figure 2f**); human CD45$^+$ chimerism

176   from the fresh group was ~3%, while 10-day and 30-day culture groups displayed ~70%

177   and ~85% chimerism, respectively (**Figure 2e**). The frequency of human CD34$^+$ cells in

178   the BM and spleen at 16- and 24-weeks was also significantly higher in the 10- or 30-day

179   culture group (**Figure 2f, Extended Data Figure 2f-g**, where multilineage output was

180   also observed (**Extended Data Table 1a**). These results confirmed that our cytokine-free

181   3a media could maintain and expand functional human HSCs for at least one-month ex

182   vivo.

183

184   ***Caprolactam polymers improve HSC growth***

185   Having established an albumin- and cytokine-free human HSC culture system,

186   we next aimed to improve the rate of HSPC expansion ex vivo. The PVA-based 3a media

187   only supported ~10-fold expansion of CD34$^+$ cells over 30 days, suggesting that further

188   improvement was required. We hypothesized that other synthetic polymers might be more

189   suitable for human HSC expansion. We therefore screened 10 polymers and identified

Soluplus®, a polyvinyl caprolactam-polyvinyl acetate-polyethylene glycol graft copolymer (PCL-PVAc-PEG) [27,28], as supportive of significantly higher cell expansion (**Figure 3a**). In PCL-PVAc-PEG-based cultures, the combination of 740Y-P, butyzamide, and UM171 was as effective as in the PVA-based cultures (**Extended Data Figure 3a-f**). However, the toxicity of SR-1 was significantly reduced compared to the PVA condition (**Extended Data Figure 3g**). PCL-PVAc-PEG-based 3a media also supported faster cell proliferation longer-term, with a ~75-fold expansion of total cells and ~55-fold expansion of CD34$^+$ cell observed after a 30-day culture (**Figure 3b**). The addition of a PI3K inhibitor led to cell death, suggesting that cell expansion was dependent on the PI3K/AKT signaling (**Extended Data Figure 3h**). Furthermore, PVA- and PCL-PVAc-PEG-based 3a media also supported ex vivo expansion of adult-PBSC CD34$^+$ cells, with a ~8-10-fold expansion of total cells observed after a 10-day culture (**Extended Data Figure 3i**).

To compare in vivo engraftment and differentiation potential of the PCL-PVAc-PEG and PVA cultured HSPCs, we performed xenotransplantation assays. We transplanted 1×10^4 cells per recipient from day-30 3a media cultures containing PVA and/or PCL-PVAc-PEG. Interestingly, similar robust human cell chimerism was observed from all conditions, including in the PB, BM, and spleen (**Figure 3c-e, Extended Data Figure 3j-l, Extended Data Table 1b, Supplementary Table 1**). Robust human CD45$^+$ chimerism was also observed in secondary xenotransplantation recipients (**Figure 3f-g, Supplementary Table 2**). However, lymphoid bias was observed due to the characteristics of the NOG mice[26,29]. We re-performed the xenotransplantation assays using human IL-3/GM-CSF-transgenic NOG (NOG IL-3/GM-Tg) mice[30]. In this context, we observed robust engraftment from long-term PCL-PVAc-PEG-based 3a cultures, with CD33$^+$ myeloid cells at 27% of human CD45$^+$ cells at 16-weeks post-transplantation (**Figure 3h, i**).

We next compared 10-day CD34$^+$ cell expansion in PCL-PVAc-PEG-based 3a media against published serum albumin-based media (StemSpan SFEM supplemented with cytokines and SR1 or UM171). While the total number of cells generated in the 10-day cultures was ~50% in 3a media (**Extended Data Figure 4a**), the frequency and absolute number of CD34$^+$EPCR$^+$CD90$^+$CD45RA$^-$ITGA3$^+$ cells was strikingly increased

221   (**Extended Data Figure 4b, c**). PCL-PVAc-PEG-based 3a media was also superior to

222   PCL-PVAc-PEG-based cytokine cocktail media (**Extended Data Figure 4b, c**).

223   Consistent with higher metabolic activity and active cell division, all culture conditions

224   caused an increase in ROS and yH2AX compared to fresh CD34$^+$ cells (**Extended Data**

225   **Figure 4d**); however, these did not accumulate further in longer-term 30-day 3a cultures

226   (**Extended Data Figure 4e**). Corresponding with the increased frequency of HSPCs, the

227   3a cultured cells also demonstrated significantly higher human CD45$^+$ PB and BM

228   chimerism following transplantation of 1x10^4 10-day cultured cells into recipient NOG

229   mice (**Extended Data Figure 4f, g**). Human CD45$^+$ chimerism was detected in the PB

230   and BM of 1/3 secondary transplantation recipients at 24-weeks post-transplantation

231   (**Extended Data Figure 4h, i**). It is worth noting that our xenotransplantation assay

232   protocol differs to those used in the development of SR-1[11], which may account for the

233   differences in engraftment. Nonetheless, these results confirmed that 3a media support

234   robust expansion of functionally engraftable human HSCs ex vivo.

235

236   ***Long-term selective HSC expansion***

237   The robust in vivo engraftment potential of these human HSC cultures suggested

238   that a high frequency of HSCs was maintained within the 3a cultures. To further

239   investigate the composition of these long-term HSPC cultures, we performed flow

240   cytometric analysis of HSC-associated surface markers. This revealed a striking

241   enrichment of phenotypic HSCs after PCL-PVAc-PEG culture, with the

242   CD34$^+$EPCR$^+$CD90$^+$CD45RA$^-$ITGA3$^+$ cell fraction significantly enriched after 7-day

243   cultures (**Extended Data Figure 4b-c, Extended Data Figure 5a**).

244   We also sought to characterize the PCL-PVAc-PEG based 3a cultures at the

245   molecular level. We performed whole exome sequencing on fresh and 10-day cultured

246   CB CD34$^+$ cells and detected seven mutations that could a cause amino acid change and

247   four mutations that were located on a splice site in cultured cells (**Extended Data Table**

248   **2**). To the best of our knowledge, these mutations are not involved in hematological

249   malignancies nor clonal hematopoiesis. These results support the safety of our culture

250   system, and suggest further clinical development is warranted.

251   We next performed bulk RNA sequencing on CD34^{high}EPCR$^+$ and

252   CD34^{high}EPCR$^-$ cells from 10-day cultures. EPCR expression is known to mark LT-HSCs

253   in UM171-supplemented media[31]. Consistent with previous studies[32], expression of LT-

254   HSC markers *HLF* and *AVP* were enriched in the CD34^{high}EPCR$^+$ fraction (**Extended**

255   **Data Figure 5b**). Additional HSC genes, *PRDM16[33]* and *FGD5[34],* were also upregulated

256   in the CD34^{high}EPCR$^+$ fraction (**Figure 4a**) and Gene Set Enrichment Analysis (GSEA)

257   confirmed that HSC gene sets were upregulated in the CD34^{high}EPCR$^+$ fraction (**Figure**

258   **4b**). GSEA also revealed that lysosomal membrane related genes were enriched in

259   CD34^{high}EPCR$^+$ cells (**Extended Data Figure 6b**), consistent with a report that lysosomal

260   activity against various external signals has an important role in the self-renewal of human

261   LT-HSCs[35]. On the other hand, oxidative phosphorylation (OXPHOS) and mitochondrial

262   ribosomes genes were upregulated in CD34^{high}EPCR$^-$ cells (**Figure 4c, Extended Data**

263   **Figure 6b**), consistent with a report that high mitochondrial membrane potential (MMP)

264   HSCs had less intracellular lysosomal contents than quiescent MMP-low LT-HSCs[36].

265   To further resolve the cellular heterogeneity within the HSC cultures, we used

266   single-cell RNA sequencing to compare our 3a conditions with StemSpan SFEM

267   supplemented with cytokines and SR1 or UM171[2,11]. After integration and analysis of

268   these three samples using Seurat, we identified and manually annotated 12 major clusters

269   (**Figure 4d, Extended Data Figure 6c**). This included a population of cells expressing

270   HSC genes, *HLF* and *AVP*, while lacking expression lineage-specific genes (*MPO,*

271   *ITGA2B*), which we termed HSPC-HLF (**Figure 4d, Extended Data Figure 6c-e**). Lower

272   expression of *HLF* and *AVP* were also seen in two other populations (HSPC, HSPC-

273   cycling), suggesting these to be intermediate stem/progenitor populations (**Extended**

274   **Data Figure 6c**). Various downstream progenitor cell types, including erythroid, MgK,

275   monocyte (Mon) and granulocyte (Gra) progenitors could also be identified (**Figure 4d,**

276   **Extended Data Figure 6c**). Comparing the cellular composition of the 3a media and

277   other two cytokine-based conditions (StemSpan SFEM with SR-1 or UM171),

278   differences were apparent. In particular, high frequencies of the HSPC-HLF cluster and

279   erythroid/MgK progenitors were observed in the 3a media, while the Mon and Gra

280   progenitor clusters were generally depleted (**Figure 4e, Extended Data Figure 6f**).

281   Similar results for the UM171 cultures were seen when we overlayed published single-

282   cell RNA-seq datasets onto our dataset (**Extended Data Figure 6g**). These results suggest

283   that 3a culture conditions were more suitable for selective expansion of LT-HSCs. These

284   differences in the cellular composition corresponded with the higher engraftment

285   potential seen in the 3a media (**Extended Data Figure 4f, g**) and confirmed the highly

286   selective nature of these cultures. In addition, 10-day cultured cells in 3a media had higher

287   levels of *HLF* expression as compared to fresh CB CD34$^+$ cell samples[32] (**Extended Data**

288   **Figure 6h**).

289   Finally, we examined whether 3a media could support the expansion of clonally-

290   derived HSC cultures. Single CB-derived CD34$^+$CD38$^-$CD90$^+$CD45RA$^-$CD49f$^+$ cells

291   were sorted into 96-well plates and cultured with PCL-PVAc-PEG-based 3a media. After

292   7 days, xenotransplantation assays were performed using NOD.Cg-

293   Prkdc^{scid}Il2rg^{tm1Sug}Kit$^{em1(V831M)Jic}$/Jic (W41/W41) recipient mice (**Figure 4f**), which

294   support higher human hematopoietic cell chimerism in xenotransplantation assays

295   (**Extended Data Figure 8**). Although heterogeneous clonal expansion was observed, 20

296   out of 96 wells (21%) expanded more than 10-fold and 11 out of 96 wells (11%) expanded

297   over 30-fold in 7 days (**Figure 4f, Supplementary Table 3**). The 10 wells with the

298   highest expansion rate were transplanted into individual recipients. Five out of the ten

299   recipients displayed robust PB, BM, and spleen chimerism with over 5% multilineage

300   human CD45$^+$ chimerism in the BM and spleen after 24-weeks (**Figure 4h, i, Extended**

301   **Data Table 1c Supplementary Table 4**). Furthermore, we performed split clone

302   experiments by transplanting single HSC-derived cultures into three W41/W41 mice

303   using HSC clones that displayed more than 10-fold expansion by day 7. For three out of

304   six clones, all three recipients showed human cell engraftment (**Extended Data Figure**

305   **7a, b**), confirming that clonal amplification of HSCs is supported by the 3a media.

306   Together, these results confirm that PCL-PVAc-PEG-based 3a media can support both

307   bulk and clonal expansion of human HSCs ex vivo.

308

309   ***Discussion***

310   Here, we report a recombinant cytokine-free albumin-free long-term expansion

311   culture system for human HSCs. These conditions selectively expanded functional

312   HSPCs for at least 30 days ex vivo and also supported clonal HSC expansion, which may

contribute to efforts to decipher the heterogeneity of the human HSC compartment in health and disease[37]. As highlighted by recent clinical trials[2,11], the ability to expand CB HSPCs ex vivo has important implications for solving the shortage of donor HSCs for allogeneic HSCT. In this regard, 3a media may hold advantages in being recombinant protein-free and chemically defined, which should improve batch-to-batch variability, reduce reagent costs and facilitate rapid clinical translation. However, further comparison of human HSC culture methods are warranted. In conclusion, this culture system provides a powerful platform for both basic scientists and clinicians interested in stem cell biology and HSC therapies.

References:

1   Copelan, E. A. Hematopoietic stem-cell transplantation. *N Engl J Med* **354**, 1813-1826, doi:10.1056/NEJMra052638 (2006).

2   Cohen, S. *et al.* Hematopoietic stem cell transplantation using single UM171-expanded cord blood: a single-arm, phase 1-2 safety and feasibility study. *Lancet Haematol* **7**, e134-e145, doi:10.1016/s2352-3026(19)30202-9 (2020).

3   Pineault, N. & Abu-Khader, A. Advances in umbilical cord blood stem cell expansion and clinical translation. *Exp Hematol* **43**, 498-513, doi:10.1016/j.exphem.2015.04.011 (2015).

4   Wilkinson, A. C. & Nakauchi, H. Stabilizing hematopoietic stem cells in vitro. *Current Opinion in Genetics & Development* **64**, 1 - 5, doi:https://doi.org/10.1016/j.gde.2020.05.035 (2020).

5   Gluckman, E. *et al.* Hematopoietic reconstitution in a patient with Fanconi's anemia by means of umbilical-cord blood from an HLA-identical sibling. *N Engl J Med* **321**, 1174-1178, doi:10.1056/nejm198910263211707 (1989).

6   Orkin, S. H. & Zon, L. I. Hematopoiesis: an evolving paradigm for stem cell biology. *Cell* **132**, 631-644, doi:10.1016/j.cell.2008.01.025 (2008).

7   Weissman, I. L. Stem cells: units of development, units of regeneration, and units in evolution. *Cell* **100**, 157-168, doi:10.1016/s0092-8674(00)81692-x (2000).

8   Wilkinson, A. C., Igarashi, K. J. & Nakauchi, H. Haematopoietic stem cell self-renewal in vivo and ex vivo. *Nat Rev Genet*, doi:10.1038/s41576-020-0241-0 (2020).

9   Boitano, A. E. *et al.* Aryl hydrocarbon receptor antagonists promote the expansion of human hematopoietic stem cells. *Science* **329**, 1345-1348, doi:10.1126/science.1191536 (2010).

10   Fares, I. *et al.* Cord blood expansion. Pyrimidoindole derivatives are agonists of human hematopoietic stem cell self-renewal. *Science* **345**, 1509-1512, doi:10.1126/science.1256337

347   (2014).

348   11   Wagner, J. E., Jr. *et al.* Phase I/II Trial of StemRegenin-1 Expanded Umbilical Cord Blood
349   Hematopoietic Stem Cells Supports Testing as a Stand-Alone Graft. *Cell Stem Cell* **18**, 144-155,
350   doi:10.1016/j.stem.2015.10.004 (2016).

351   12   Bai, T. *et al.* Expansion of primitive human hematopoietic stem cells by culture in a zwitterionic
352   hydrogel. *Nat Med* **25**, 1566-1575, doi:10.1038/s41591-019-0601-5 (2019).

353   13   Grey, W. *et al.* Activation of the receptor tyrosine kinase RET improves long-term hematopoietic
354   stem cell outgrowth and potency. *Blood* **136**, 2535-2547, doi:10.1182/blood.2020006302 (2020).

355   14   Huang, J., Nguyen-McCarty, M., Hexner, E. O., Danet-Desnoyers, G. & Klein, P. S. Maintenance
356   of hematopoietic stem cells through regulation of Wnt and mTOR pathways. *Nat Med* **18**, 1778-
357   1785, doi:10.1038/nm.2984 (2012).

358   15   Wilkinson, A. C. *et al.* Long-term ex vivo haematopoietic-stem-cell expansion allows
359   nonconditioned transplantation. *Nature* **571**, 117-121, doi:10.1038/s41586-019-1244-x (2019).

360   16   Wilkinson, A. C., Ishida, R., Nakauchi, H. & Yamazaki, S. Long-term ex vivo expansion of mouse
361   hematopoietic stem cells. *Nat Protoc* **15**, 628-648, doi:10.1038/s41596-019-0263-2 (2020).

362   17   Ieyasu, A. *et al.* An All-Recombinant Protein-Based Culture System Specifically Identifies
363   Hematopoietic Stem Cell Maintenance Factors. *Stem Cell Reports* **8**, 500-508,
364   doi:10.1016/j.stemcr.2017.01.015 (2017).

365   18   Seita, J. *et al.* Lnk negatively regulates self-renewal of hematopoietic stem cells by modifying
366   thrombopoietin-mediated signal transduction. *Proc Natl Acad Sci U S A* **104**, 2349-2354,
367   doi:10.1073/pnas.0606238104 (2007).

368   19   Park, H. J. *et al.* Cytokine-induced megakaryocytic differentiation is regulated by genome-wide
369   loss of a uSTAT transcriptional program. *EMBO J* **35**, 580-594, doi:10.15252/embj.201592383
370   (2016).

371   20   Yamazaki, S. *et al.* Cytokine signals modulated via lipid rafts mimic niche signals and induce
372   hibernation in hematopoietic stem cells. *Embo j* **25**, 3515-3523, doi:10.1038/sj.emboj.7601236
373   (2006).

374   21   Miyamoto, K. *et al.* Foxo3a is essential for maintenance of the hematopoietic stem cell pool. *Cell*
375   *Stem Cell* **1**, 101-112, doi:10.1016/j.stem.2007.02.001 (2007).

376   22   Tadokoro, Y. *et al.* Spred1 Safeguards Hematopoietic Homeostasis against Diet-Induced Systemic
377   Stress. *Cell Stem Cell* **22**, 713-725.e718, doi:10.1016/j.stem.2018.04.002 (2018).

378   23   Lechman, E. R. *et al.* Attenuation of miR-126 activity expands HSC in vivo without exhaustion.
379   *Cell Stem Cell* **11**, 799-811, doi:10.1016/j.stem.2012.09.001 (2012).

380   24   Sakurai, M., Takemoto, H., Mori, T., Okamoto, S. & Yamazaki, S. In vivo expansion of functional
381   human hematopoietic stem progenitor cells by butyzamide. *Int J Hematol*, doi:10.1007/s12185-
382   020-02849-2 (2020).

383 25 Nishimura, T. *et al.* Use of polyvinyl alcohol for chimeric antigen receptor T-cell expansion. *Exp*
384   *Hematol* **80**, 16-20, doi:10.1016/j.exphem.2019.11.007 (2019).

385 26 Ito, M. *et al.* NOD/SCID/gamma(c)(null) mouse: an excellent recipient mouse model for
386   engraftment of human cells. *Blood* **100**, 3175-3182, doi:10.1182/blood-2001-12-0207 (2002).

387 27 Linn, M. *et al.* Soluplus® as an effective absorption enhancer of poorly soluble drugs in vitro and
388   in vivo. *Eur J Pharm Sci* **45**, 336-343, doi:10.1016/j.ejps.2011.11.025 (2012).

389 28 Jin, X., Zhou, B., Xue, L. & San, W. Soluplus(®) micelles as a potential drug delivery system for
390   reversal of resistant tumor. *Biomed Pharmacother* **69**, 388-395, doi:10.1016/j.biopha.2014.12.028
391   (2015).

392 29 Sudo, K., Yamazaki, S., Wilkinson, A. C., Nakauchi, H. & Nakamura, Y. Polyvinyl alcohol
393   hydrolysis rate and molecular weight influence human and murine HSC activity ex vivo. *Stem Cell*
394   *Res* **56**, 102531, doi:10.1016/j.scr.2021.102531 (2021).

395 30 Ito, R. *et al.* Establishment of a human allergy model using human IL-3/GM-CSF-transgenic NOG
396   mice. *J Immunol* **191**, 2890-2899, doi:10.4049/jimmunol.1203543 (2013).

397 31 Fares, I. *et al.* EPCR expression marks UM171-expanded CD34(+) cord blood stem cells. *Blood*
398   **129**, 3344-3351, doi:10.1182/blood-2016-11-750729 (2017).

399 32 Lehnertz, B. *et al.* HLF expression defines the human hematopoietic stem cell state. *Blood* **138**,
400   2642-2654, doi:10.1182/blood.2021010745 (2021).

401 33 Aguilo, F. *et al.* Prdm16 is a physiologic regulator of hematopoietic stem cells. *Blood* **117**, 5057-
402   5066, doi:10.1182/blood-2010-08-300145 (2011).

403 34 Che, J. L. C. *et al.* Identification and characterization of in vitro expanded hematopoietic stem
404   cells. *EMBO Rep* **23**, e55502, doi:10.15252/embr.202255502 (2022).

405 35 García-Prat, L. *et al.* TFEB-mediated endolysosomal activity controls human hematopoietic stem
406   cell fate. *Cell Stem Cell* **28**, 1838-1850.e1810, doi:10.1016/j.stem.2021.07.003 (2021).

407 36 Liang, R. *et al.* Restraining Lysosomal Activity Preserves Hematopoietic Stem Cell Quiescence
408   and Potency. *Cell Stem Cell* **26**, 359-376.e357, doi:10.1016/j.stem.2020.01.013 (2020).

409 37 Lee-Six, H. *et al.* Population dynamics of normal human blood inferred from somatic
410   mutations. *Nature* **561**, 473-478, doi:10.1038/s41586-018-0497-0 (2018).

411 38 Subramanian, A. *et al.* Gene set enrichment analysis: a knowledge-based approach for interpreting
412   genome-wide expression profiles. *Proc Natl Acad Sci U S A* **102**, 15545-15550,
413   doi:10.1073/pnas.0506580102 (2005).

414

Figure Legends:

416 *Figure 1. Chemically-defined cytokine-free media maintains human hematopoietic*

417 *stem/progenitor cells (HSPCs) ex vivo*

418 **(a)** Ex vivo proliferation of 1000 mouse bone marrow (BM) c-Kit$^+$Sca-1$^+$Linage$^-$ (KSL)

419 HSPCs or 1000 human cord blood-derived (CB) CD34$^+$CD38$^-$ HSPCs cultured with 10

420 ng/ml SCF and 100 ng/ml THPO in polyvinyl alcohol (PVA)-based media. Mean of five

421 independent cultures. **P = 0.0034; ***P = 0.0001; ****P < 0.0001.

422 **(b)** Single cell phosphorylation status of PI3K and AKT in mouse KSL and human CB

423 CD34$^+$CD38$^-$ cultured with PVA-based media containing SCF and THPO. Mean of 30

424 cells. AFI: average fluorescence intensity. ****P < 0.0001.

425 **(c)** Fold change in total cell numbers of human-cord-blood-derived CD34$^+$CD38$^-$ cultured

426 with SC79 or 740Y-P in addition to human 10 ng/ml SCF (S) and 100 ng/ml THPO (T)

427 in PVA-based media conditions. The starting cell count was 1000. Mean of five

428 independent cultures. *P = 0.0145; **P = 0.0051.

429 **(d)** Fold change in total and CD34$^+$ cell numbers after a 7-day culture of 2x10^4 human

430 CB CD34$^+$ cells in PVA-based media containing 740Y-P and 100 ng/ml THPO (T) with

431 or without 10 ng/ml SCF (S). Mean of three independent cultures.

432 **(e)** Fold change in total and CD34$^+$ cell numbers after a 7-day culture of 2x10^4 of human

433 CB CD34$^+$ cells in PVA-based media containing 740Y-P and THPO (T) or butyzamide

434 (Buty). Mean of three independent cultures. **$^†P$ = 0.0020; **$^‡P$ = 0.0054.

435 **(f)** Fold change in total and CD34$^+$ cell number after a 7-day culture of 2x10^4 human CB

436 CD34$^+$ cells in PVA-based media containing 0-20 μM 740Y-P and 0.01-0.5 μM

437 butyzamide. Mean of three independent cultures.

438 **(g)** Cell numbers and phenotypes during the culture of 2.5x10^3 human CB CD34$^+$ cells in

439 PVA-based media containing 1 μM 740Y-P and 0.1 μM butyzamide. Mean ± S.D. of

440 three independent cultures.

441 Statistical significance was calculated using an unpaired two-tailed *t*-test: n.s., not

442 significant.

443 *Figure 2. Long-term ex vivo expansion of human HSPCs in chemically-defined*
444 *cytokine-free cultures*

445 (**a**) Fold change in total and CD34$^+$ cell numbers after a 7-day culture of 2x10^4 human
446 CB CD34$^+$ cells in PVA-based media containing 750 nM SR-1 and/or 70 nM UM171 in
447 addition to 2a media containing 1 μM 740Y-P and 0.1 μM butyzamide. Mean of three
448 independent cultures. **$P = 0.0095$.

449 (**b**) Total, CD34$^+$, and CD41$^+$ cell numbers after a 14-day culture of 2x10^4 CB CD34$^+$
450 cells in PVA-based 2a media with or without 70 nM UM171. Mean of three independent
451 cultures. ***$P = 0.004$; ****$P < 0.0001$.

452 (**c**) Fold change in total and CD34$^+$ cell numbers during a 30-day culture of 2x10^4 CB
453 CD34$^+$ cells in PVA-based media containing 1 μM 740Y-P, 0.1 μM butyzamide, and 70
454 nM UM171 (PVA-based 3a media). Mean of three independent cultures.

455 (**d**) Mean human CD45$^+$ PB chimerism in recipient NOG mice at 4-, 8- and 12-weeks
456 following transplantation of 1x10^4 fresh CB CD34$^+$ cells or the cells derived from a 10-
457 day or 30-day culture of 1x10^4 CB CD34$^+$ cells in PVA-based 3a media. n=5-6 mice per
458 group. *$P = 0.0401$; ***$P = 0.0001$; ****$P < 0.0001$.

459 (**e**) Mean 16-week human CD45$^+$ cell chimerism in the BM and spleen from mice
460 described in (**d**). n=3 mice per group. ***$P = 0.0003$; ****$P < 0.0001$.

461 (**f**) Mean 16-week human CD34$^+$ cell chimerism in the BM and spleen from mice
462 described in (**d**). n=3 mice per group. *$^†P = 0.0116$; *$^‡P = 0.0416$; .**$P = 0.0055$.

463 Statistical significance was calculated using an unpaired two-tailed *t*-test or ANOVA. n.s.,
464 not significant.

Figure 3. Caprolactam polymer-based 3a media supports efficient human HSC expansion ex vivo

(**a**) Total cell numbers generated after 7-days culture of $2x10^4$ human CB CD34$^+$ cells in 3a media containing various synthetic polymers (see in ***Methods*** for details). No polymer (none) was used as a negative control. Mean $\pm$ S.D. of three independent cultures. n.d., not detected.

(**b**) Fold change in total and CD34$^+$ cell numbers during a 30-day culture of $2x10^4$ CB CD34$^+$ in 3a media containing PVA and/or polyvinyl caprolactam-polyvinyl acetate-polyethylene glycol graft copolymer (PCL-PVAc-PEG). Mean of three independent cultures. $*P = 0.0170$; $**^\dagger P = 0.0190$; $**^\ddagger P = 0.0012$; $**^\S P = 0.0013$; $**^\| P = 0.0023$; $***P = 0.0006$.

(**c**) Mean human CD45$^+$ PB chimerism in recipient NOG mice following transplantation of $1x10^4$ day-30 cells derived from CB CD34$^+$ cell cultured in 3a media containing PVA or PCL-PVAc-PEG (cultures initiated with $1x10^4$ cells). n=5 per group. Results from replicate experiments shown in **Supplementary Table 1**. Independent experiments performed with 2-3 human CB samples per experiment. $*P = 0.0424$.

(**d, e**) Mean 16-week human CD45$^+$ and CD34$^+$ cell chimerism in the BM and spleen from mice described in (**c**). n=5 per group.

(**f, g**) Mean human CD45$^+$ PB, BM and spleen chimerism in secondary recipient NOG mice following transplantation of $1x10^6$ cells derived from primary recipients, as describe in (**d, e**). n=5 per group. Results from replicate experiments shown in **Supplementary Table 2**.

(**h**) Human PB chimerism and phenotypes in humanized IL-3/GM-CSF-transgenic NOG mice at 16-weeks following transplantation of $1x10^4$ day-20 cells derived from CB CD34$^+$ cell cultured in 3a media containing PCL-PVAc-PEG (cultures initiated with $1x10^4$ cells). n=5 per group. $****P < 0.0001$.

(**i**) Frequency for each human CD45$^+$ cell subpopulation in the PB from mice described in (**h**). Mean $\pm$ S.D. of five mice per group.

Statistical significance was calculated using an unpaired two-tailed *t*-test: n.s., not significant.

Figure 4. Long-term selective expansion of functional human HSCs in 3a media

(a) Log_2-fold expression change of indicated HSC-associated genes. Mean $\pm$ S.D. of three independent cultures. EPCR$^+$ and EPCR$^-$ indicates CD34^{high}EPCR$^+$ cells and CD34^{high}EPCR$^-$ cells, respectively. **†*P* = 0.0049; **‡*P* = 0.0043; **§*P* = 0.0022; ***P = 0.0006.

(b, c) Results from gene set enrichment analysis (GSEA) for genes differentially expressed between CD34^{high}EPCR$^+$ and CD34^{high}EPCR$^-$ samples using gene sets for HSC genes **(b)** and mitochondrial oxidative phosphorylation-related genes **(c)**. Statistical significance was calculated using an empirical phenotype-based permutation test procedure[38].

(d) UMAP plot of single-cell RNA sequencing data from 10-day expanded CD34$^+$ CB cells with 12 cell clusters annotated (see in ***Methods*** for details). Integrated cell map from cells cultured in PCL-PVAc-PEG based 3a media, StemSpan with SR-1 media, or StemSpan with UM171 media. Statistical significance was calculated using an empirical phenotype-based permutation test procedure[38].

(e) Cell distribution within PCL-PVAc-PEG based 3a cultures, StemSpan with SR-1 cultures, and StemSpan with UM171 cultures. Black dotted frames indicate the HSPC-HLF cell cluster. See **Extended Data Figure 6g** for a quantification of *HLF* expression.

(f) Schematic of the single HSC expansion assay.

(g) Mean number of cells derived from single human CD34$^+$CD38$^-$CD90$^+$CD45RA$^-$CD49f$^+$ CB cell after 7-days culture (n=96). Results from replicate experiments shown in **Supplementary Table 3**. Independent experiments performed with 2-3 human CB samples per experiment.

(h, i) Mean human CD45$^+$ PB and BM chimerism in recipient NOD.Cg-Prkdc^{scid} Il2rg^{tm1Sug} Kit$^{em1(V831M)Jic}$/Jic (W41/W41) mice following transplantation (n=10), as described in **(g)**. Results from replicate experiments shown in **Supplementary Table 4**. Statistical significance was calculated using an unpaired two-tailed *t*-test.

Methods:

Mice. C57BL/6 mice were purchased from Sankyo Lab Service (Tsukuba, Japan) or bred in-house. Immunodeficient NOD/Shi-scid, IL-2Rγ[null] (NOG), NOD.Cg-Prkdc[scid] Il2rg[tm1Sug] Kit[em1(V831M)Jic]/Jic (W41/W41), and human IL-3/GM-CSF-transgenic NOG (NOG IL-3/GM-Tg) mice[30] were purchased from the Central Institute for Experimental Animals (Kanagawa, Japan).

NOG and W41/W41 mice were developed at the Central Institute for Experimental Animals. Kit-mutated NOG-W41 mice were established by genome editing using transcription activator-like effector nucleases (TALENs). Designed TALEN mRNA pairs (Forward; 5'-gtgttccgttctaggcac-3', and Reverse; 5'-atgctctctggtgccatc-3') and 100-bp single-strand oligonucleotide (ssOligo) containing a G to A point mutation in the kinase domain of the c-Kit locus[39] were purchased from Thermo Fisher Scientific (Waltham, MA, USA). TALEN mRNA (4 ng/µl) and ssOligo (15 ng/µl) were mixed and injected into NOG mouse embryo to generate NOG-W41 mice. All mice were housed in specific-pathogen-free conditions with free access to food and water. All animal experiments were performed in accordance with institutional guidelines and were approved by the Animal Care and Use Committee of the Institute of Medical Science, The University of Tokyo, the Laboratory Animal Resource Center, University of Tsukuba and the Institutional Animal Care and Use Committee of Central Institute for Experimental Animals.

Isolation of mouse cells. Bone marrow (BM) c-Kit[+]Sca-1^{+}Lineage[-] (KSL) cells were isolated from 8- to 12-week-old mice. Whole BM cells were stained with APC-conjugated anti-c-Kit antibody (eBioscience, San Diego, CA, USA) and c-Kit^{+} cells enriched using anti-APC magnetic beads and LS columns (Miltenyi Biotec). The c-Kit-enriched cells were then stained with PE-conjugated anti-Sca-1 (eBioscience), and a lineage antibody cocktail (biotinylated CD4, 1:200, CD8, 1:200, CD45R, 1:200, TER119, 1:100, LY-6G/LY-6C 1:200, and CD127; 1:100, all from eBioscience), followed by staining with FITC-CD34 and streptavidin-APC-eFluor 780 (eBioscience, 1:200). Cell populations were purified and sorted by FACS AriaII (BD Biosciences,

554 Franklin Lakes, NJ, USA) with BD FACS Diva software using propidium iodide as a

555 dead cell stain. Antibodies are described in **Supplementary Table 5.**

556

557 ***Human umbilical cord blood cells.*** Human umbilical cord blood-derived (CB) CD34$^+$

558 cells were purchased from StemExpress (Folsom, CA, USA). CD34$^+$CD38$^-$ cells were

559 purified by staining thawed CD34$^+$ cells with PE-Cy7-labeled anti-human CD34 (BD

560 Biosciences, 1:100) and V450-labeled anti-human CD38 (BD Biosciences, 1:100), then

561 sorted as described above. For detailed phenotypic HSC analysis, cells were stained with

562 PerCP-Cy5.5-labeled anti-human CD34 (BioLegend, San Diego, CA, USA, 1:100),

563 BV421-labeled anti-human CD38 (BD Biosciences, 1:100), PE-Cy7-labeled anti-human

564 CD90 (BD Biosciences, 1:100), APC-H7-labeled anti-human CD45RA (BD Biosciences,

565 1:100) and PE-labeled anti-human CD49f (BD Biosciences, 1:100), then sorted as

566 described above. Antibodies are described in **Supplementary Table 5.** For all

567 experiments, different lots of CBs were used. For the comparison of fresh and expanded

568 cells, a common lot of cord blood was used.

569

570 ***PVA and cytokine-based cell cultures.*** Human CB CD34$^+$ cells cultures were performed

571 using IMDM (Life Technologies, Carlsbad, CA, USA), 1% insulin-transferrin-selenium-

572 ethanolamine (ITSX; Life Technologies), 1% penicillin/streptomycin/glutamine (P/S/G;

573 Life Technologies), 0.1% Good Manufacturing Practice Grade polyvinyl alcohol (PVA;

574 Japan VAM&POVAL CO., LTD, Osaka, Japan), 10 ng/ml recombinant human SCF

575 (PeproTech, Rocky Hill, NJ, USA) and 100 ng/ml recombinant human THPO

576 (PeproTech), at 37°C with 5% CO$_2$. Cultures were supplemented with 740Y-P (CAS No.

577 236188-16-1; synthesized) and SC79 (CAS No. 305834-79-1; Sigma-Aldrich, St. Louis,

578 MO, USA), as indicated. Mouse cell cultures were performed using F12 media (Life

579 Technologies), 1% ITSX, 1% P/S/G, 10 mM HEPES (Life Technologies), 0.1% PVA, 10

580 ng/ml recombinant mouse SCF (PeproTech) and 100 ng/ml recombinant mouse THPO

581 (PeproTech), at 37°C with 5% CO$_2$. U-bottomed 96-well tissue culture plates were used

582 in mouse and human comparative experiments. All other cultures were performed using

583 24-well flat-bottomed CellBIND® tissue culture plates (Corning, Corning, NY, USA;

584 Product Number 3337).

585

Signaling analysis. Phosphorylation status of signaling molecules was analyzed by fluorescent immunocytostaining. At indicated timepoints, cells were attached to poly-l-lysine-coated slides (Matsunami Glass, Osaka, Japan), then fixed with 4% paraformaldehyde and permeabilized with 0.1% Triton X-100. The cells were stained with phosphorylation-specific anti-PI3K, anti-Stat5, anti-AKT, anti-JAK2, anti-Stat3, anti-p38MAPK, and anti-p44/42MAPK antibodies (all from Thermo Fisher Scientific, Waltham, MA, USA). After washing with PBS, cells were stained with Alexa Fluor 488-conjugated goat anti-rabbit IgG antibody (CAS No. A11008, Invitrogen) and DAPI. Immunofluorescence images were obtained and analyzed using a Cellomics ArrayScan VTI HCS Reader (Thermo Scientific) as described previously[18,40]. All experiments were performed using mixture of five cord blood samples.

PVA-based cytokine-free cultures. Human CB CD34^{+} cell cultures were performed using IMDM, 1% ITSX, 1% P/S/G, 0.1% PVA, 740Y-P and butyzamide (Shionogi, Osaka, Japan) at 37 °C with 5% CO_2. All long-term cultures used 1 μM 740Y-P and 0.1 μM butyzamide, with media changes made every 3 days by manually removing conditioned media by pipetting and replacing pre-warmed and freshly prepared media. Butyzamide is a THPO receptor agonist[41,42] and has also been used clinically as a lusutrombopag. All cell cultures were performed using 24-well flat-bottomed CellBIND® tissue culture plates. Where indicated, cultures were supplemented with 750 nM StemRegenin 1 (SR-1; CAS No. 1227633-49-9) and/or 70 nM UM171 (CAS No. 1448724-09-1). As described in the main text, we defined media containing 1 μM 740Y-P, 0.1 μM butyzamide and 70 nM UM171 as 3a media.

PCL-PVAc-PEG-based cytokine-free cultures. A step-by-step protocol describing the culture of human CB CD34^{+} cells with PCL-PVAc-PEG-based cytokine-free media can be found at Protocol Exchange[43]. Human CB CD34^{+} cell cultures were performed using IMDM, 1% ITSX, 1% P/S/G, 1 μM 740Y-P, 0.1 μM butyzamide and 0.1% of polyvinyl caprolactam-polyvinyl acetate-polyethylene glycol graft copolymer (PCL-PVAc-PEG; Soluplus®; BASF, Ludwigshafen am Rhein, Germany) at 37 °C with 5% CO_2. For long-

term cultures, media changes made every 3 days by manually removing conditioned media by pipetting and replacing pre-warmed and freshly prepared media. For polymer screening, human CB CD34$^+$ cells were cultured with IMDM, 1% ITSX, 1% P/S/G, 1 µM 740Y-P, 0.1 µM butyzamide and 0.1% one of the following chemicals: PVA, 188 BIO (Kolliphor® P 188 Bio; BASF), 188 Geismar (Kolliphor® P188; BASF), PCL-PVAc-PEG, 407 Geismar (Kolliphor® P407; BASF), 30 Geismar (Kollidon® 30, BASF), 17 PF (Kollidon® 17 PF; BASF), 90 F (Kollidon® 90 F; BASF) or 12 PF (Kollidon® 12 PF; BASF) at 37 °C with 5% CO_2. In addition, PCL-PVAc-PEG-based cytokine cocktails media consisted of 10 ng/ml recombinant mouse SCF (PeproTech) and 100 ng/ml recombinant mouse THPO (PeproTech) (described in **Extended Data Figure 4a**).

UM171 and/or SR-1-based cultures. Human CB CD34$^+$ cell cultures for xenotransplantation assays were performed using StemSpan SFEM (Stem Cell Technologies, Vancouver, BC, Canada) supplemented with 100 ng/ml recombinant human SCF (PeproTech), 100 ng/ml FMS-like tyrosine kinase 3 ligand (FLT3, PeproTech), 50 ng/ml recombinant human THPO (PeproTech), 10 µg/ml lipoproteins (Stem Cell Technologies) and 35nM UM171 and/or 750nM SR-1 at 37 °C with 5% CO_2 (**Extended Data Figure 4f-i**) [10]. In comparison experiments with previously protocols, human CB CD34$^+$ cell cultures were performed using StemSpan SFEM supplemented with 50 ng/ml recombinant human SCF (PeproTech), 50 ng/ml FLT3-L, 50 ng/ml recombinant human THPO, 50 ng/ml recombinant human IL-6 (PeproTech) and 750nM SR-1 at 37 °C with 5% CO_2 (described in **Figure 4e**, **Extended Data Figure 4a-e, Extended Data Figure 5a, Extended Data Figure 6g**) [11].

Analysis of cell cultures. Cultured cells were counted using a hemocytometer or a CYTORECON cytometer (GE Healthcare, Amersham, UK) before and after culture. Phenotypic analysis was performed by staining cells with PE-Cy7-labeled anti-human CD34 (1:100), V450-labeled anti-human CD38 and FITC-labeled anti-human CD41 (BioLegend, 1:100), followed by flow cytometric analysis using a FACS AriaII or FACS Verse (BD Biosciences) with BD FACS Diva software using propidium iodide as a dead stain. For detailed phenotypic HSC analysis, fresh or cultured cells were stained with

647   PerCP-Cy5.5-labeled anti-human CD34 (BioLegend, 1:100), BV421-labeled anti-human

648   CD38 (BD Biosciences, 1:100), PE-Cy7-labeled anti-human CD90 (BD Biosciences,

649   1:100), APC-H7-labeled anti-human CD45RA (BD Biosciences, 1:100), PE-labeled anti-

650   human CD49f (BD Biosciences, 1:100), FITC-labeled anti-human lineage cocktail (CD2,

651   CD3, CD4, CD7, CD8, CD10, CD11b, CD14, CD19, CD20, CD56, CD235a) (BD

652   Biosciences, 1:200) and FITC-labeled (BioLegend, 1:200) or BV711-labeled (BD

653   Biosciences, 1:100) anti-human CD41, followed by flow cytometric analysis using a

654   FACS AriaIII (BD Biosciences) with BD FACS Diva software using propidium iodide

655   as a dead stain. As a set of markers containing EPCR, cultured cells were stained with

656   APC-labeled anti-human CD34 (BioLegend, 1:100), BV421-labeled anti-human CD90

657   (BioLegend, 1:100), PerCP-Cy5.5-labeled anti-human CD45RA (BioLegend, 1:20), PE-

658   labeled anti-human CD49c (ITGA3) (BD Biosciences, 1:200), BV605-labeled anti-

659   human CD201 (EPCR) (BD Biosciences, 1:100) and FITC-labeled anti-human lineage

660   cocktail. Antibodies are described in **Supplementary Table 5.** Results were analyzed

661   with FlowJo software 10.8.1 (Tree Star, Ashland, OR).

662

663   ***Colony forming unit (CFU) assays.*** Defined numbers of fresh or cultured cells were

664   sorted by FACS AriaII and subjected to CFU assays using Methocult H4435 (Stem Cell

665   Technologies). Cells were incubated in a humidified atmosphere at 37 °C with 5% CO_2.

666   After two weeks, the number of colonies were counted and types of colonies were

667   validated by cytospin smears stained with Hemacolor (Merck, Darmstadt, Germany).

668

669   ***Xenotransplantation assays.*** Fresh or cultured human CB CD34$^+$ cells were transplanted

670   by tail artery injection[44] into sub-lethally (1.5 Gy) irradiated 8-10-week-old

671   immunodeficient NOD/Shi-scid IL-2Rγ^{null} (NOG) mice or NOG IL-3/GM-Tg mice.

672   Human cell chimerism in the peripheral blood analyzed using V450–labeled anti-mouse

673   CD45.1 (BD Biosciences, 1:200) and APC-Cy7–labeled anti-human CD45 antibodies

674   (BioLegend, 1:100) following red blood cell lysis. Mice were randomly selected and BM

675   and spleen analysis was performed. Human CD34$^+$ cell chimerism in the BM and spleen

676   was determined using V450–labeled anti-mouse CD45.1 (1:200), APC-Cy7–labeled anti-

677   human CD45 antibodies (1:100), and PE–labeled anti-human CD34 (BioLegend, 1:50).

678 For detailed phenotypic HSC analysis, cells were stained with PerCP-Cy5.5-labeled anti-
679 human CD34 (BioLegend, 1:100), BV421-labeled anti-human CD38 (BD Biosciences,
680 1:100), PE-Cy7-labeled anti-human CD90 (BD Biosciences, 1:100), APC-H7-labeled
681 anti-human CD45RA (BD Biosciences, 1:100) and PE-labeled anti-human CD49f (BD
682 Biosciences, 1:100)**.** Human lineage chimerism in the BM and spleen was determined
683 using V450–labeled anti-mouse CD45.1, APC-Cy7–labeled anti-human CD45 antibodies,
684 PE-Cy7-labeled anti-human CD33 (eBioscience, 1:20), PE-labeled anti-human CD3
685 (eBioscience, 1:20), and APC–labeled anti-human CD19 (eBioscience, 1:100). We
686 defined CD33$^+$ cells as myeloid cells, CD19$^+$ cells as B cells, and CD3$^+$ cells as T cells.
687 In xenotransplantation assays using NOG IL-3/GM-Tg mice (described in **Figure 3h, i**),
688 we used PE-labeled anti-human CD56 (BioLegend, 1:100) and FITC-labeled anti-human
689 CD66b (BioLegend, 1:100) additionally. Flow cytometry analysis was then performed
690 using a FACS AriaII or FACS Verse (BD Biosciences) with propidium iodide as dead
691 stain, and results were analyzed with FlowJo software. For secondary transplantation
692 assays, we collected and pooled bone marrow from all primary recipient mice at 16 weeks
693 and transplanted 1x10^6 cells into each sub-lethally-irradiated NOG mice as described
694 above, with donor chimerism analyzed as above. In xenotransplantation assays using
695 W41/W41 and NOG mice (described in **Extended Data Figure 8**), 5x10^4 fresh human
696 CB CD34$^+$ cells were transplanted into W41/W41, W41/+ or +/+ mice with or without
697 irradiation, with donor chimerism analyzed as above.

698

699 ***Clonal HSC expansion assays.*** Single human CB-derived CD34$^+$CD38$^-$CD90$^+$CD45RA$^-$
700 CD49f$^+$ cells were purified by staining thawed PerCP-Cy5.5-labeled anti-human CD34
701 (BioLegend, 1:100), BV421-labeled anti-human CD38 (BD Biosciences, 1:100), PE-
702 Cy7-labeled anti-human CD90 (BD Biosciences, 1:100), APC-H7-labeled anti-human
703 CD45RA (BD Biosciences, 1:100) and PE-labeled anti-human CD49f (BD Biosciences,
704 1:100) then sorted single cell into a 96-well flat-bottomed CellBIND® tissue culture plate.
705 After culturing with PCL-PVAc-PEG-based 3a media for 7 days as described above, the
706 top 10 wells with high expansion efficiency were transplanted into sub-lethally (1 Gy)
707 irradiated 8-10-week-old W41/W41 mice by tail artery injection (detailed in **Figure 4f**).
708 For split clone transplantation assays, after culturing with PCL-PVAc-PEG-based 3a

709   media for 7 days as described above, each of the 6 wells with highest expansion efficiency

710   were transplanted into three sub-lethally (1 Gy) irradiated 8-10-week-old W41/W41 mice

711   by tail artery injection (detailed in **Extended Data Figure 7a, b**).

712

713   ***Thrombopoietin receptor agonist screening.*** MPL-expressing 32D cells culture were

714   performed using RPMI media containing 1% ITSX, 1% P/S/G, and 0.1% BSA or PVA at

715   37 °C with 5% CO_2. One of the following thrombopoietin receptor agonists was added to

716   each culture: 7 µM eltrombopag (Cayman Chemical Company, Ann Arbor, MI, USA); 3

717   µM avatrombopag (MedChemExpress, Monmouth Junction, NJ, USA); or 0.1 µM

718   butyzamide[41]. Human CB CD34^{+} cell cultures were performed using IMDM, 1% ITSX,

719   1% P/S/G, 0.1% PVA, 740Y-P, and one of the following thrombopoietin receptor agonist:

720   7 µM eltrombopag, 3 µM avatrombopag, or 0.1 µM butyzamide at 37 °C with 5% CO_2.

721

722   ***Preparation and culture of human peripheral blood stem cells.*** Fresh human peripheral

723   blood stem cells (PBSCs) were obtained from healthy adult donors for allogeneic

724   transplantation in the University of Tsukuba Hospital (approval R02-009). The donors

725   received the treatment of G-CSF before leukapheresis. All donors agreed to experimental

726   use of their PBSCs after informed consent and our study was approved by the ethical

727   committee in the University of Tsukuba. From PBSCs, mononuclear cells (MCs) were

728   separated by Lymphocytes Separation Medium 1077 (PromoCell, CAS No. C-44010).

729   After separation, CD34^{+} cells were enriched using the Human CD34 Microbeads Kit

730   (Miltenyi Biotec Inc., CAS No. 130-046-702) and MACS LS columns (Miltenyi Biotec

731   Inc., CAS No. 130-042-401). Purified CD34^{+} cells were cultured in PVA- and PCL-

732   PVAc-PEG based 2a or 3a media. In 3a media cultures, UM729 (1 µM) was used in place

733   of UM171 because UM171 was not commercially available at the time this experiment

734   was performed. All experiments complied with all relevant guidelines and regulations.

735

736   ***Exome Sequencing.*** We extracted genomic DNA of fresh and 10-day cultured human

737   CB CD34^{+} cells using QIAamp DNA Blood Mini Kit (QIAGEN, CAS No. 51106). After

738   DNA fragmentation, target enrichment by hybrid capture probes was performed using

739   SureSelect Human All Exon V6 (Agilent). Enriched DNA was sequenced on NovaSeq

740   6000 (Macrogen Inc, Korea). FASTQ files were imported to CLC Genomics Workbench

741   (ver. 10.1.1) for subsequent analysis. Sequence data was annotated using the reference

742   genome (GRCh38). After filtering out common variants using the database of Tohoku

743   Medical Megabank Organization (https://www.megabank.tohoku.ac.jp), we annotated

744   mutations unique to the culture sample that were located in amino-acid change sites or

745   splicing sites.

746

747   ***Bulk RNA sequencing.*** Human CB CD34$^+$ cells were cultured in PCL-PVAc-PEG based

748   3a media at 37°C with 5% CO_2 for 10-days. CD34^{high}EPCR$^+$ and CD34^{high}EPCR$^-$ cells

749   were then sorted by MoFlo XDP (Beckman Coulter) and processed in TRIZOL-LS

750   (Thermo Fisher Scientific, 10296028). Total RNA was used for rRNA-depletion by

751   NEBNExt rRNA Depletion Kit (New England Biolabs, CAS No. E6310), and next

752   directional library synthesis by NEBNext Ultra Directional RNA Library Prep Kit for

753   Illumina (New England Biolabs, CAS No. E7420). Libraries were sequenced on Illumina

754   NextSeq 5000. We analyzed the data using the edgeR v3.14[45] in R (4.1.1). Volcano plots

755   were   generated   using   EnhancedVolcano

756   (https://github.com/kevinblighe/EnhancedVolcano) in R and genes highlighted when the

757   value of $\log_2$ fold change was >2 and $-\log_{10}P$ was >14. Gene Ontology enrichment

758   analysis was performed by ClusterProfiler[46]. Gene set enrichment analysis (GSEA)

759   software (http://www.gsea-msigdb.org/gsea/index.jsp) was used for comparing our

760   datasets with two previously published datasets.

761

762   ***Single-cell RNA sequencing.*** Human CB CD34$^+$ cells were cultured for 10-days at 37°C

763   with 5% CO_2 under three different conditions as follows: (1) PCL-PVAc-PEG based 3a

764   media (composition described above); (2) StemSpan SFEM (Stem Cell Technologies,

765   Vancouver, BC, Canada) supplemented with 100 ng/ml recombinant human SCF

766   (PeproTech), 100 ng/ml FMS-like tyrosine kinase 3 ligand (FLT3, PeproTech), 50 ng/ml

767   recombinant human THPO (PeproTech), 10 µg/ml lipoproteins (Stem Cell Technologies)

768   and 35 nM UM171[2]; and (3) StemSpan SFEM supplemented with 50 ng/ml recombinant

769   human SCF (PeproTech), 50 ng/ml FLT3-L, 50 ng/ml recombinant human THPO, 50

770   ng/ml recombinant human IL-6   (PeproTech) and 750 nM SR-1[11]. From each CB cell

771   culture, the propidium iodide-negative fraction was sorted by MoFlo (Beckman Coulter)

772   and single cell Gel Beads-in-Emulsions were generated using the Chromium Controller

773   (10x Genomics). Libraries were generated using the Single Cell 3' Reagent Kit version

774   3.1 (10x Genomics) according to manufacturer's instructions.

775   Cells were sequenced on Illumina Hiseq X (Macrogen Inc, Korea). Sequence data

776   was annotated by the reference genome (GRCh38) using the Cellranger v6.1.1 pipeline.

777   Subsequent analysis was performed using Seurat v4.047 in R. Using the Read10X

778   function, we obtained the unique molecular identified (UMI) count matrix of each dataset.

779   This analysis identified 9913 cells for the PCL-PVAc-PEG sample, 5912 cells for the

780   UM171 sample, and 9198 cells for the SR-1 sample. The mean reads per cell was 32205

781   for the PCL-PVAc-PEG sample, 36026 for the UM171 sample, and 30991 for the SR-1.

782   The median number of genes detected per cell was 3292 genes for the PCL-PVAc-PEG

783   sample, 3648 genes for the UM171 sample, and 3300 genes for the SR-1 sample. We

784   filtered out cells that had unique feature counts of over 7500 or less than 200, and cells

785   with >10% mitochondrial counts. The filtered cell count number (cells used for

786   subsequent analysis) was 9572 cells for the PCL-PVAc-PEG sample, 5373 cells for the

787   UM171 sample, and 6991 cells for the SR-1 sample, with 22179 features, 21222 features,

788   and 21645 features detected, respectively.

789   Normalization and scaling were performed with the SCTransform function

790   (method = "glmGamPoi"). At this time, the effect of the mitochondrial gene expression

791   ratio was removed (var.to.regress = "percent.mt"). The SelectIntegrationFeatures

792   (nfeatures = 3000) function was used to select genes for integration of the datasets. After

793   processing the datasets with the PrepSCTIntegration function, FindIntegrationAnchors

794   and IntegrateData functions were used to find anchors for integration and integrate the

795   datasets. To correct for cell-to-cell variation due to the effects of cell cycle, cell cycle

796   scoring and regression was performed with CellCycleScoring function, using a published

797   mouse hematopoietic stem cells dataset[47]. Scaling was then performed with the ScaleData

798   (vars.to.regress = c("S.Score", "G2M.Score")) function. Principal components analysis

799   (PCA) was performed using the RunPCA function (npc = 30). Uniform Manifold

800   Approximation and Projection (UMAP) was performed using the RunUMAP function to

801   reduce the dimension of the dataset of embedded cells into two dimensions.

802   FindNeighbors function was used to determine k-nearest neighbors (KNN) for each cell,
803   and the KNN graph was constructed based on Euclidean distance. Finally, processed cells
804   were clustered based on KNN using the Louvain algorithm (resolution = 0.4) by the
805   FindCluster function. FindMarkers and FindAllMarkers functions were used to identify
806   intercluster differentially expressed genes and select feature genes that characterized
807   specific hematopoietic cell types. This allowed for the follow clusters to be manually
808   annotation: hematopoietic stem/progenitor cells highly expressing *HLF* (HSPC-HLF),
809   hematopoietic stem/progenitor cells (HSPC), cell-cycle activated hematopoietic
810   stem/progenitor cells (HSPC-Cycling), granulocyte-monocyte progenitor cells (GMP),
811   monocyte progenitor cells (MP), granulocyte progenitor cells (GP), dendritic cell
812   progenitors (DCP), CD34 and *GATA2*-expressing progenitor cells (CD34$^+$GATA2$^+$ prog),
813   megakaryocyte and erythroid progenitor cells (MEP), erythroid progenitor cells (EryP),
814   megakaryocyte progenitor cells (MgkP), and mast cell progenitors (MCP).

815   Subsequent analysis was performed using Seurat v4.0[48] in R. Fresh CB data for
816   the comparison of *HLF* expression in cultured cells (**Extended Data Figure 6g**) was
817   obtained from GEO (GSE 153370)[32].   In addition, we compared our datasets with GEO-
818   deposited scRNAseq data from 7-day cultured CB CB34$^+$ cells in StemSpan SFEM +
819   UM171 (GSE 153370). We filtered out cells (with feature counts over 7500 or less than
820   200, and those with >10% mitochondrial counts) and used NormalizedData,
821   CellCycleScoring and ScaleData functions to process data. Next, FindTransferAnchors
822   was performed to find anchors between our datasets (as reference data) and the published
823   datasets (as query data). After the RunUMAP function (reduction.model = TRUE) was
824   applied to the reference data, MapQuery function was used to perform Unimodal UMAP
825   Projection (**Extended Data Figure 6f**).

826

827   ***Cell Cycle analysis.*** Cultured human CB CD34$^+$ cells were stained with APC-labeled
828   anti-human CD34 (BioLegend), PerCP-Cy5.5-labeled anti-human CD45RA (BioLegend),
829   then washed with phosphate-buffered saline (PBS) twice and pelleted. BD
830   Cytofix/Cytoperm Fixation/Permeabilization Kit (BD Biosciences, 554714) was then
831   used to process the samples according to manufacturer's instructions. After fixation and
832   permeabilization, the cells were stained with FITC-labeled anti-human Ki67 (BioLegend,

833   1:100) and DAPI (DOJINDO, 1:1000). FITC-labeled IgG2b kappa (BioLegend, 1:100)

834   was used as an isotype control. Antibodies are described in **Supplementary Table 5.**

835   Analysis was performed on a LSR Fortessa Cell Analyzer (BD Bioscience). Data was

836   analyzed with FlowJo software.

837

838   ***Apoptosis assay.*** Suspension of cultured human CB CD34$^+$ cells were centrifuged and

839   washed by PBS. Next, annexin binding buffer (10mM HEPES, 140mM NaCl and 2.5mM

840   CaCl$_2$ diluted in distilled water) was added to the sample. After that, the cells were stained

841   by AlexaFluor488 AnnexinV (Invitrogen, 1:40) and propidium iodide

842   (BioLegend1:1000) and incubated for 15 minutes at room temperature. Antibodies are

843   described in **Supplementary Table 5.** Finally, we resuspended the samples in the annexin

844   binding buffer and analyzed them by LSR Fortessa Cell Analyzer (BD Biosciences).

845

846   ***Reactive Oxygen Species (ROS) Assay.*** Fresh and cultured cells were pre-stained with

847   APC-labeled anti-human CD34 (BioLegend, 343510). The cells were then processed with

848   a ROS Assay Kit-Photo-oxidation Resistant DCFH-DA (DOJINDO, R253) according to

849   the manufacturer's instructions. Cell samples were incubated in the Working Buffer for

850   30 minutes at 37°C with 5% CO$_2$ and then washed with HBSS twice. Analysis was

851   performed on a Attune NxT Flow Cytometer (Invitrogen). Data was analyzed with

852   FlowJo software.

853

854   ***γH2A.X Assay.*** Fresh and cultured cells were pre-stained with APC-labeled anti-human

855   CD34 (BioLegend, 343510). The cells were then processed with BD Cytofix/Cytoperm

856   Fixation/Permeabilization Kit (BD Biosciences, 554714) according to the manufacturer's

857   instructions and intracellularly stained with FITC-labeled anti-H2A.X Phospho (Ser139)

858   antibody (BioLegend, 613404, 1:100). Analysis was performed on a Attune NxT Flow

859   Cytometer (Invitrogen). Data was analyzed with FlowJo software.

860

861   ***Statistical analysis.*** Statistical analysis was performed using two-tailed t-testing or

862   ANOVA in Prism 9 software (GraphPad, San Diego, CA, USA).

Additional references:

39   Nocka, K. *et al.* Molecular bases of dominant negative and loss of function mutations at the murine c-kit/white spotting locus: W37, Wv, W41 and W. *Embo j* **9**, 1805-1813 (1990).

40   Ema, H. *et al.* Adult mouse hematopoietic stem cells: purification and single-cell assays. *Nat Protoc* **1**, 2979-2987, doi:10.1038/nprot.2006.447 (2006).

41   Nogami, W. *et al.* The effect of a novel, small non-peptidyl molecule butyzamide on human thrombopoietin receptor and megakaryopoiesis. *Haematologica* **93**, 1495-1504, doi:10.3324/haematol.12752 (2008).

42   Sakurai, M., Takemoto, H., Mori, T., Okamoto, S. & Yamazaki, S. In vivo expansion of functional human hematopoietic stem progenitor cells by butyzamide. *Int J Hematol* **111**, 739-741, doi:10.1007/s12185-020-02849-2 (2020).

43   Sakurai, M., Ishitsuka, K. & Yamazaki, S. Cytokine-free ex vivo expansion of human hematopoietic stem cells. *Protoc. Exch.*

44   Kuchimaru, T. *et al.* A reliable murine model of bone metastasis by injecting cancer cells through caudal arteries. *Nat Commun* **9**, 2981, doi:10.1038/s41467-018-05366-3 (2018).

45   Robinson, M. D., McCarthy, D. J. & Smyth, G. K. edgeR: a Bioconductor package for differential expression analysis of digital gene expression data. *Bioinformatics* **26**, 139-140, doi:10.1093/bioinformatics/btp616 (2010).

46   Wu, T. *et al.* clusterProfiler 4.0: A universal enrichment tool for interpreting omics data. *Innovation (N Y)* **2**, 100141, doi:10.1016/j.xinn.2021.100141 (2021).

47   Nestorowa, S. *et al.* A single-cell resolution map of mouse hematopoietic stem and progenitor cell differentiation. *Blood* **128**, e20-31, doi:10.1182/blood-2016-05-716480 (2016).

48   Hao, Y. *et al.* Integrated analysis of multimodal single-cell data. *Cell* **184**, 3573-3587.e3529, doi:10.1016/j.cell.2021.04.048 (2021).

909

910 **Author contributions:** M.S., K.I. and S.Y. conceived, designed and performed

911 experiments, analyzed data and wrote the paper. R.I., T.K., E.M., H.N., K.S., H.J.B. and

912 H.T. designed and performed experiments. M.S. performed cell cultures, colony-forming

913 unit assays and FACS analysis, and xenotransplantation assays. K.I. performed cell

914 cultures, FACS analysis, exome sequencing, RNA sequencing, cell cycle analysis,

915 apoptosis assays, ROS assays, and γH2A.X assays, S.Y performed cell cultures, signaling

916 analysis, xenotransplantation assays, and clonal HSC expansion assays, R.I. performed

917 xenotransplantation assays, T.K. performed exome sequencing and RNA sequencing,

918 E.M., H.N, K.S. H.J.B. and H.T. helped with cell cultures and FACS analysis. S.Y.

919 performed independent replications of the experiments (Supplementary Table 1-4) both

920 in the University of Tokyo, University of Tsukuba, and R.I. performed independent

921 replications of the experiment (Supplementary Table 1-2) in Central Institute for

922 Experimental Animals. A.C.W. and D.G.K. analyzed data and wrote the paper. T.S.

923 provided reagents and discussed the results. K.K., S.T., Y.N., A.I., S.C. and S.O.

924 discussed the results and wrote the paper. H.N. guided and supervised the project. All

925 authors edited and approved the paper.

926

927 **Competing interests:** M.S and S.Y are co-founders and shareholders in Celaid
928 Therapeutics. H.N. is a co-founder and shareholder in Megakaryon, Century Therapeutics
929 and Celaid Therapeutics. All other authors declare no competing interests.
930
931 **Supplementary Information:** This file contains Supplementary Tables 1-5.
932
933 **Materials and Correspondence:** Satoshi Yamazaki, y-sato4@md.tsukuba.ac.jp;
934 Hiromitsu Nakauchi, nakauchi@stanford.edu
935
936 **Extended data figures and tables:** 8 Extended Data Figures and 2 Extended Data Tables
937 available in the online version of the paper.
938

Extended Data Figure Legends:

Extended Data Figure 1: Development of chemically-defined cytokine-free culture media for human hematopoietic stem/progenitor cells (HSPCs)

(a) Single cell phosphorylation status of JAK2, STAT3, STAT5, p38 MAPK, and p44/42 MAPK in mouse KSL and human CB CD34$^+$CD38$^-$ cells cultured with 10 ng/ml SCF and 100 ng/ml THPO in PVA-based media. Mean of 30 cells. AFI: average fluorescence intensity. ****$P < 0.0001$.

(b) Representative image of p-PI3K after 7-days culture cells in mouse and human, as described in (a). Blue: DAPI, Green：anti-PI3K. Scale bar: 100 μm.

(c) Single cell phosphorylation status of PI3K in mouse CD34$^-$KSL and human CD34$^+$CD38$^-$CD90$^+$CD45RA$^-$CD49f$^+$ CB cells cultured with 10 ng/ml SCF and 100 ng/ml THPO in PVA-based media for 3 and 7 days. Mean of 31 cells. AFI: average fluorescence intensity. ****$P < 0.0001$.

(d) CD34$^+$CD45RA$^-$ cell numbers of human-cord-blood-derived CD34$^+$CD38$^-$ cultured with SC79 or 740Y-P in addition to human 10 ng/ml SCF (S) and 100 ng/ml THPO (T) in PVA culture conditions for 7 days. The starting cell count was 2x10^4. Mean of three independent cultures. **$P = 0.0040$.

(e) Single cell phosphorylation status of PI3K in human CD34$^+$CD38$^-$CD90$^+$CD45RA$^-$CD49f$^+$ CB cells cultured in PVA-based media containing 10 ng/ml SCF and 100 ng/ml THPO with or without 740Y-P for 7 days. Mean of 31 cells. AFI: average fluorescence intensity. ***$P = 0.0002$.

(f) Cell cycle analysis of CD34$^+$CD45RA$^-$ cells after a 7-day culture of human CB CD34$^+$ cells in PVA-based media containing 740Y-P and 100 ng/ml THPO (T) with or without 10 ng/ml SCF (S). Mean of three independent cultures. Representative FACS plot was shown on the right.

(g) Fold change in GEmM colony numbers generated from human CB CD34$^+$ cells after a 7-day culture in PVA-based media supplemented with 740Y-P and THPO (T) with or without SCF (S), relative to fresh CD34$^+$ cells. Mean of three independent cultures.

(h) Total cell numbers after 1x10^3 MPL-expressing 32D cells (32D/MPL) were cultured for 3-days with various THPO agonists (eltrombopag, avatrombopag or butyzamide) in BSA-based or PVA-based media. Mean of two independent cultures. n.d., not detected.

(i) Fold change in total and CD34$^+$ cell numbers after a 7-day culture of $2\text{x}10^4$ CD34$^+$ cells in PVA-based media supplemented with 740Y-P and various THPO agonists (eltrombopag, avatrombopag or butyzamide). Mean of three independent cultures. n.d., not detected.

(j) CD34$^+$ CD41$^-$ CD90$^+$CD45RA$^-$ cell numbers after a 7-day culture of $2\text{x}10^4$ of human CB CD34$^+$ cells in PVA-based media containing 740Y-P and 100 ng/ml THPO (T) and/or butyzamide (Buty). Mean of three independent cultures. **$P = 0.0020$; ***$P = 0.0010$.

(k) Fold change in GEmM colony numbers generated from CD34$^+$ cells after a 7-day culture in PVA-based media supplemented with 740Y-P and THPO (T) or butyzamide (Buty), relative to fresh CD34$^+$ cells. Mean $\pm$ S.D. of three independent cultures. **$P = 0.0017$.

(l) The frequency of cells during the culture of $2\text{x}10^4$ human CB CD34$^+$ cells in PVA-based media containing 1 µM 740Y-P and 0.1 µM butyzamide. Mean $\pm$ S.D. of three independent cultures.

(m) Representative image of a day-14 PVA-based culture containing 1 µM 740Y-P and 0.1 µM butyzamide (2a media). Representative of at least five experiments. Scale bar: 100 µm.

(n) Megakaryocytic (MgK) colony numbers obtained from 50 CD34$^+$ cells sorted from day 7 and day 14 PVA-based cultures containing 1 µM 740Y-P and 0.1 µM butyzamide (2a media). Mean $\pm$ S.D. of three independent cultures. *$P = 0.0161$.

(o, p) Mean human CD45$^+$ peripheral blood (PB) and BM chimerism in recipient NOD/Shi-scid IL-2Rγ^{null} (NOG) mice following transplantation of $1\text{x}10^4$ cells derived from a 7-day or 14-day culture of $1\text{x}10^4$ CB CD34$^+$ cells in PVA-based 2a media containing 1 µM 740Y-P and 0.1 µM butyzamide. n=5 mice per group. **(o)** **$^\dagger P = 0.0036$; **$^\ddagger P = 0.0037$; ***$P = 0.0007$, **(p)*****$P = 0.0003$.

Statistical significance was calculated using an unpaired two-tailed t-test. n.s., not significant.

Extended Data Figure 2: Long-term ex vivo expansion of human HSPCs in chemically-defined cytokine-free cultures

(a) CD34$^+$ EPCR$^+$ cell numbers after a 7-day culture of 2x10^4 human CB CD34$^+$ cells in PVA-based media containing 750 nM SR-1 and/or 70 nM UM171 in addition to 2a media. Mean of three independent cultures. ****$P < 0.0001$.

(b) CD34$^+$ EPCR$^+$ and CD34$^+$EPCR$^+$CD90$^+$CD45RA$^-$ITGA3$^+$ cell numbers after a 14-day culture of 2x10^4 CB CD34$^+$ cells in PVA-based 2a media with or without 70 nM UM171. Mean of three independent cultures. ****$P < 0.0001$.

(c) The frequency of CD34$^+$EPCR$^+$CD90$^+$CD45RA$^-$ITGA3$^+$ cells after a 10-day culture of 2x10^4 human CB CD34$^+$ cells in StemSpan SFEM supplemented with cytokines with 35 nM UM171 and PVA-based 2a media with 35 or 70 nM UM171. Mean of three independent cultures. ****$P < 0.0001$.

(d) Annexin V staining assay of total cells after a 7-day culture of 2x10^4 human CB CD34$^+$ cells in PVA-based media containing 750 nM SR-1 and/or 0.1% BSA in addition to 2a or 10 ng/ml SCF (S) and 100 ng/ml THPO (T). Mean of three independent cultures. ****$P < 0.0001$.

(e) Mean human CD45$^+$ PB chimerism in recipient NOG mice at 24 weeks following transplantation of 1x10^4 fresh CB CD34$^+$ cells or the cells derived from a 10-day or 30-day culture of 1x10^4 CB CD34$^+$ cells in PVA-based 3a media. n=3 mice per group. Details described in **Figure 2d**. *$^†P = 0.0495$; *$^‡P = 0.0319$.

(f) Mean 24-week human CD45$^+$, CD34$^+$, CD34$^+$CD38$^-$CD90$^+$CD45RA$^-$CD49f$^+$ cell chimerism in the BM from mice described in (e). n=3 mice per group. Details described in **Figure 2d.** *$^†P = 0.0112$; *$^‡P = 0.0480$; *$^§ P = 0.0187$; **$P = 0.0075$; ***$P = 0.0003$; ****$P < 0.0001$.

(g) Mean 24-week human CD45$^+$, CD34$^+$, CD34$^+$CD38$^-$CD90$^+$CD45RA$^-$CD49f$^+$ cell chimerism in the spleen from mice described in (e). n=3 mice per group. Details described in **Figure 2d.** **$P = 0.0014$.

Statistical significance was calculated using one-way ANOVA or an unpaired two-tailed *t*-test. n.s., not significant.

Extended Data Figure 3: Caprolactam polymer-based 3a media supports efficient expansion of human HSCs ex vivo

1030   **(a)** CD34$^+$CD45RA$^-$ cell numbers of human-cord-blood-derived CD34$^+$ cultured with

1031   SC79 or 740Y-P in addition to human 10 ng/ml SCF (S) and 100 ng/ml THPO (T) in

1032   PCL-PVAc-PEG culture conditions for 7 days. The starting cell count was 2x10^4. Mean

1033   of three independent cultures. *P = 0.0210.

1034   **(b)** CD34$^+$CD41$^-$CD90$^+$CD45RA$^-$ cell numbers after a 7-day culture of 2x10^4 human CB

1035   CD34$^+$ cells in PCL-PVAc-PEG-based media containing 740Y-P and 100 ng/ml THPO

1036   (T) and/or butyzamide (Buty). Mean of three independent cultures. *P = 0.0256.

1037   **(c)** CD34$^+$EPCR$^+$ and CD34$^+$EPCR$^+$CD90$^+$CD45RA$^-$ cell numbers after a 7-day culture

1038   of 2x10^4 human CB CD34$^+$ cells in PCL-PVAc-PEG -based 2a media containing 750 nM

1039   SR-1 and/or 70 nM UM171 . Mean of three independent cultures. **P = 0.0021; ***P =

1040   0.0002.

1041   **(d)** CD34$^+$CD41$^-$CD90$^+$CD45RA$^-$ cell numbers after a 7-day culture of 2x10^4 of human

1042   CB CD34$^+$ cells in PCL-PVAc-PEG-based media containing 0-20 μM, 740Y-P, and 0.1

1043   μM butyzamide. Mean of three independent cultures. *$^†P$ = 0.0214; *$^‡P$ = 0.0440.

1044   **(e)** The frequency of CD34$^+$EPCR$^+$CD90$^+$CD45RA$^-$ITGA3$^+$ cells after a 7-day culture of

1045   2x10^4 human CB CD34$^+$ cells in PCL-PVAc-PEG-based 2a media with 35 nM or 70 nM

1046   UM171. Mean of three independent cultures.

1047   **(f)** GEmM colony numbers generated from CD34$^+$ cells after a 10-day culture in PVA-

1048   and/or PCL-PVAc-PEG-based 3a media. Mean of three independent cultures. ***P =

1049   0.0005.

1050   **(g)** Annexin V staining assay of total cells after a 7-day culture of 2x10^4 human CB CD34$^+$

1051   cells in PVA- or PCL-PVAc-PEG-based 2a media containing 750 nM SR-1. Mean of

1052   three independent cultures. **P = 0.0086.

1053   **(h)** The frequency of PI positive cells after a 7-day culture of 2x10^4 human CB CD34$^+$

1054   cells in PCL-PVAc-PEG-based 3a media with or without 10 μM LY294002 (Chemscene,

1055   CAS No. 154447-36-6), PI3-kinase inhibitor. Mean of three independent cultures. ****P

1056   < 0.0001.

1057   **(i)** Total and CD34$^+$EPCR$^+$CD90$^+$CD45RA$^-$ITGA3$^+$ cell numbers after a 10-day culture

1058   of 2x10^4 adult-peripheral blood stem cell (PBSC) CD34$^+$ cells in PVA- or PCL-PVAc-

1059   PEG-based 3a media including UM729 instead of UM171. Mean of three independent

1060   cultures. *P=0.0153, **P=0.0079.

(j) Mean human CD45$^+$ PB chimerism in recipient NOG mice at 24 weeks after transplantation of 1x10^4 day-30 cells derived from CB CD34$^+$ cells cultured in 3a media containing PVA or PCL-PVAc-PEG. n=3 mice per group. Detailed described in **Figure 3c.**

(k) Mean 24-week human CD45$^+$, CD34$^+$, CD34$^+$CD38$^-$CD90$^+$CD45RA$^-$CD49f$^+$ cell chimerism in the BM from mice described in (**j**). n=3 mice per group. Detailed described in **Figure 3c.**

(l) Mean 24-week human CD45$^+$, CD34$^+$, CD34$^+$CD38$^-$CD90$^+$CD45RA$^-$CD49f$^+$ cell chimerism in the spleen from mice described in (**j**). n=3 mice per group. Detailed described in **Figure 3c.**

Statistical significance was calculated using one-way ANOVA or an unpaired two-tailed *t*-test: n.s., not significant.

Extended Data Figure 4: Comparison of human HSC culture protocols

(a) Total cell numbers generated from a 10-day culture of 2x10^4 human CB CD34$^+$ cells in PCL-PVAc-PEG or StemSpan SFEM-based cytokine-cocktail media with UM171 and/or SR-1 (see in ***Methods*** for details), or PCL-PVAc-PEG-based 3a media. Mean of three independent cultures. ***P = 0.0002; ****P <0.0001.

(b) The frequency and **(c)** absolute number of CD34$^+$EPCR$^+$CD90$^+$CD45RA$^-$ITGA3$^+$ cells in cultures described in (**a**). Mean of three independent cultures. **(b)** ****P <0.0001. **(c)** **P = 0.0010; ***†*P* = 0.0009; ***‡*P* = 0.0002; ****P <0.0001.

(d) The ROS and γH2AX level of fresh CB CD34$^+$ cells (fresh) and CD34$^+$ cells in cultures described in (**a**). Mean of three independent cultures. **P = 0.0028; ***P = 0.0004; ****P <0.0001.

(e) Relative mean fluorescence intensity (MFI) for ROS and yH2AX in fresh CB CD34$^+$ cells (fresh) and cells from 10 or 30 day PCL-PVAc-PEG-based 3a media cultures. Mean of three independent cultures.

(f, g) Mean human CD45$^+$ PB and BM chimerism in recipient NOG mice following transplantation of 1x10^4 day-10 cells derived cultures as describe in (**a**). n=4 mice per group. ***P = 0.0001; ****P <0.0001.

1091   (**h, i**) Mean human CD45$^+$ PB and BM chimerism in secondary recipient NOG mice

1092   following transplantation of 1x10^6 BM cells derived from primary recipient mice, as

1093   describe in (**f, g**). n=3 mice per group. *$^†P$ = 0.0180; *$^‡P$ = 0.0299.

1094   Statistical significance was calculated using one-way ANOVA: n.s., not significant.

1095

1096   ***Extended Data Figure 5: Gating strategy for HSCs fraction by flow cytometry***

1097   (**a**) FACS gating strategy for detecting CD34$^+$EPCR$^+$CD90$^+$CD45RA$^-$ITGA3$^+$ cells after

1098   10-day culture in 3a media containing PCL-PVAc-PEG or using UM171/SR-1.

1099

1100   ***Extended Data Figure 6: Profile of human HSCs expanded in 3a media***

1101   (**a**) Volcano plot showing differentially expressed genes (DEGs) detected in bulk RNA-

1102   sequencing of CD34^{high}EPCR$^+$ (right) and CD34^{high}EPCR$^-$ (left) cells after 10-day culture

1103   in PCL-PVAc-PEG based 3a media. DEGs are highlighted as red dots (log$_2$FC >2, -log$P$

1104   Value <14). Gene names are shown in the boxes.

1105   (**b**) GO Term cellular component-specific GSEA analysis performed on DEGs, displayed

1106   as a dotplot.

1107   (**c**) Expression of key genes within annotated clusters, displayed as a dotplot.

1108   (**d, e**) Feature plots showing *HLF* (c) and *AVP* (d) gene expression within the integrated

1109   cell map.

1110   (**f**) Ratio of each cell cluster within PCL-PVAc-PEG based 3a cultures, StemSpan with

1111   SR-1 cultures, and StemSpan with UM171 cultures, as described in **Figure 4e**.

1112   (**g**) Comparison of scRNAseq data from cells cultured for 10 days in PCL-PVAc-PEG

1113   based 3a media with two dataset of cells cultured for 7 days in StemSpan SFEM with

1114   UM171 cultures obtained from GEO (GSE 153370).

1115   (**h**) Violin plots displaying *HLF* expression in cells from a 10-day culture using 3a media,

1116   cells from UM171/SR-1 cultures, and two fresh CBs from publicly available data (GSE

1117   153370).

1118

1119   ***Extended Data Figure 7: Split clone assays***

1120   (**a**) Schematic of assay of the single HSC expansion and split clone assay. Single human

1121   CD34$^+$CD38$^-$CD90$^+$CD45RA$^-$CD49f$^+$ CB cells were sorted into 96 wells and expanded

1122 in 3a media containing PCL-PVAc-PEG for 7 days. Individual HSC clones were then

1123 transplanted into three recipient W41/W41 mice.

1124 **(b)** Human CD45$^+$ PB chimerism in recipient W41/W41 mice 24 weeks after

1125 transplantation of day-7 cells derived from single human CD34$^+$CD38$^-$CD90$^+$CD45RA$^-$

1126 CD49f$^+$ CB cell cultured in 3a media containing PCL-PVAc-PEG (3 mice/well), as

1127 described in **(a)**.

1128

1129 *Extended Data Figure 8: NOG-W41/W41 mice display high human hematopoietic cell*

1130 *chimerism*

1131 **(a)** Mean human CD45$^+$ PB chimerism in recipient NOD.Cg-Prkdc^{scid} Il2rg^{tm1Sug}

1132 Kit$^{em1(V831M)Jic}$/Jic (W41/W41), W41/+, +/+ mice at 4, 8, 12, 16 and 20 weeks following

1133 transplantation of 5x10^4 fresh CB CD34$^+$ cells. n=3-4 mice per group. ***P = 0.0004;

1134 ****P <0.0001.

1135 **(b)** Mean 24-week human CD45$^+$ cell chimerism in the BM and spleen from mice

1136 described in **(a)**. n=3-4 mice per group. **†*P* = 0.0016; **‡*P* = 0.0021; ***†*P* = 0.0001;

1137 ***‡*P* = 0.0006.

1138 **(c)** Mean human CD45$^+$, CD19$^+$, CD33$^+$, CD3$^+$, CD56$^+$ and CD66b$^+$ PB chimerism in

1139 recipient non-irradiated or irradiated (0.5 Gy) W41/W41 mice at 4-, 8-, 12- and 16-weeks

1140 following transplantation of 5x10^4 fresh CB CD34$^+$ cells. Mean $\pm$ S.D of 3-4 mice per

1141 group. *†*P* = 0.0257; *‡*P* = 0.0335; **†*P* = 0.0030; **‡*P* = 0.0060; ***P = 0.0002.

1142 Statistical significance was calculated using one-way ANOVA or an unpaired two-tailed

1143 *t*-test: n.s., not significant.

1144

1145 *Extended Data Table 1: Detailed data of xenotransplantation assays*

1146 **(a)** Mean $\pm$ S.D 16-week frequency of CD33$^+$ myeloid cells, CD3$^+$ T cells, and CD19$^+$ B

1147 cells of human CD45$^+$ cells in the BM and spleen of mice described in **Figure 2e**.

1148 **(b)** Mean $\pm$ S.D 16-week frequency of CD33$^+$ myeloid cells, CD3$^+$ T cells, and CD19$^+$ B

1149 cells of human CD45$^+$ cells in the BM and spleen of mice described in **Figure 3d.**

1150 **(c)** Mean $\pm$ S.D 24-week frequency of CD33$^+$ myeloid cells, CD3$^+$ T cells, and CD19$^+$ B

1151 cells of human CD45$^+$ cells in the PB of mice described in **Figure 4i**.

1152

1153 ***Extended Data Table 2: Whole exome sequencing on uncultured and 10-day cultured***

1154 ***cells.*** Whole exome sequencing on fresh CB and 10-day cultured CB CD34+ cells with
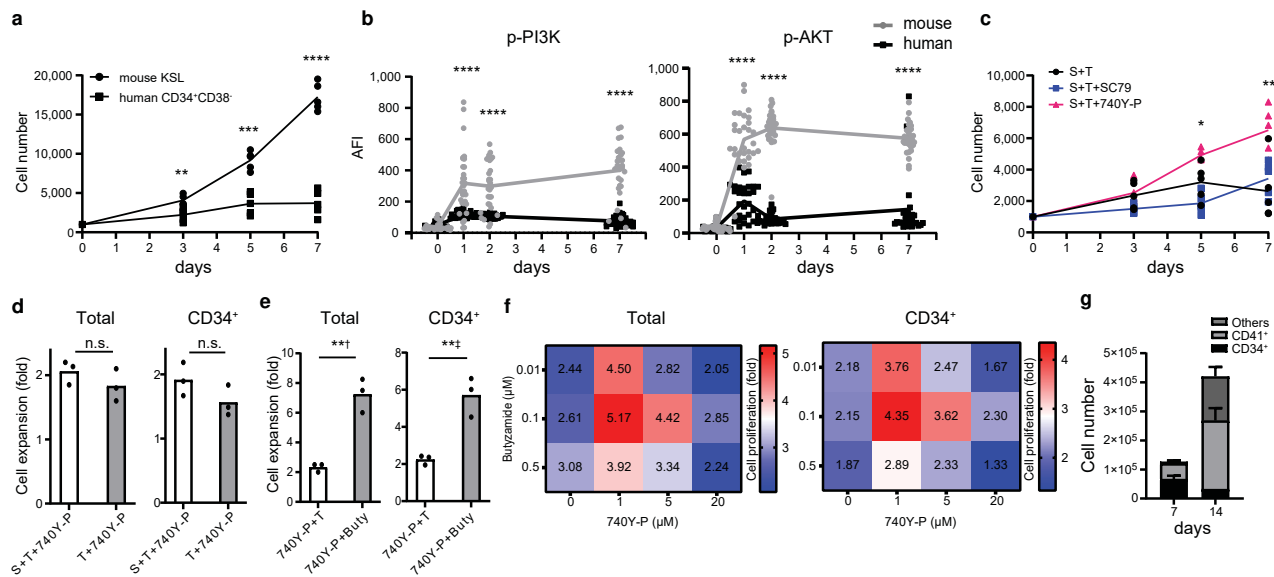
1155 PCL-PVAc-PEG-based 3a medium.
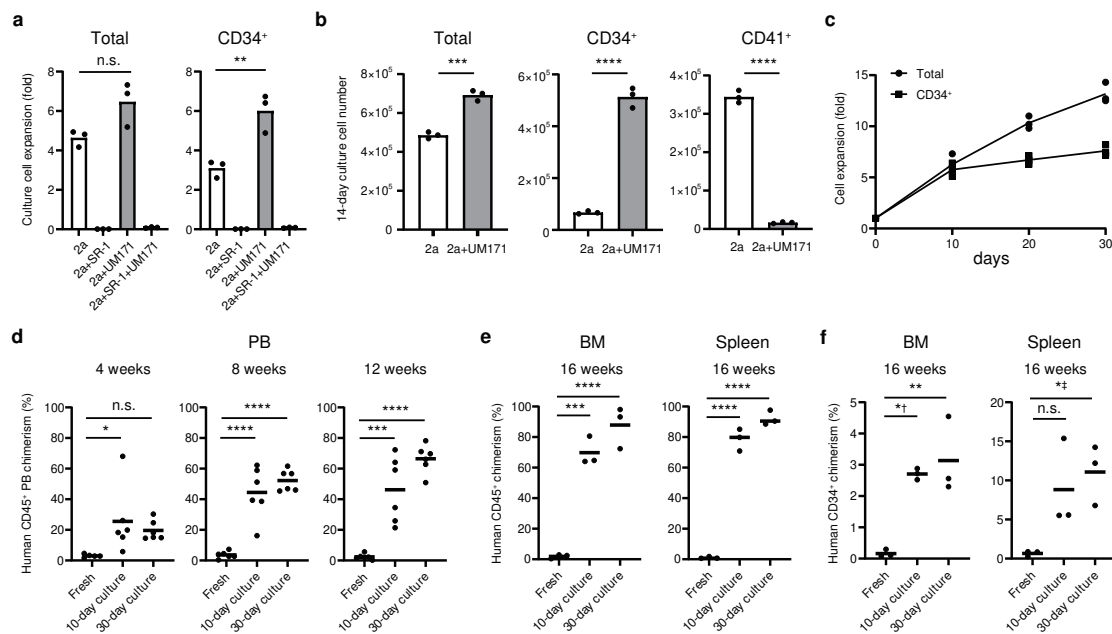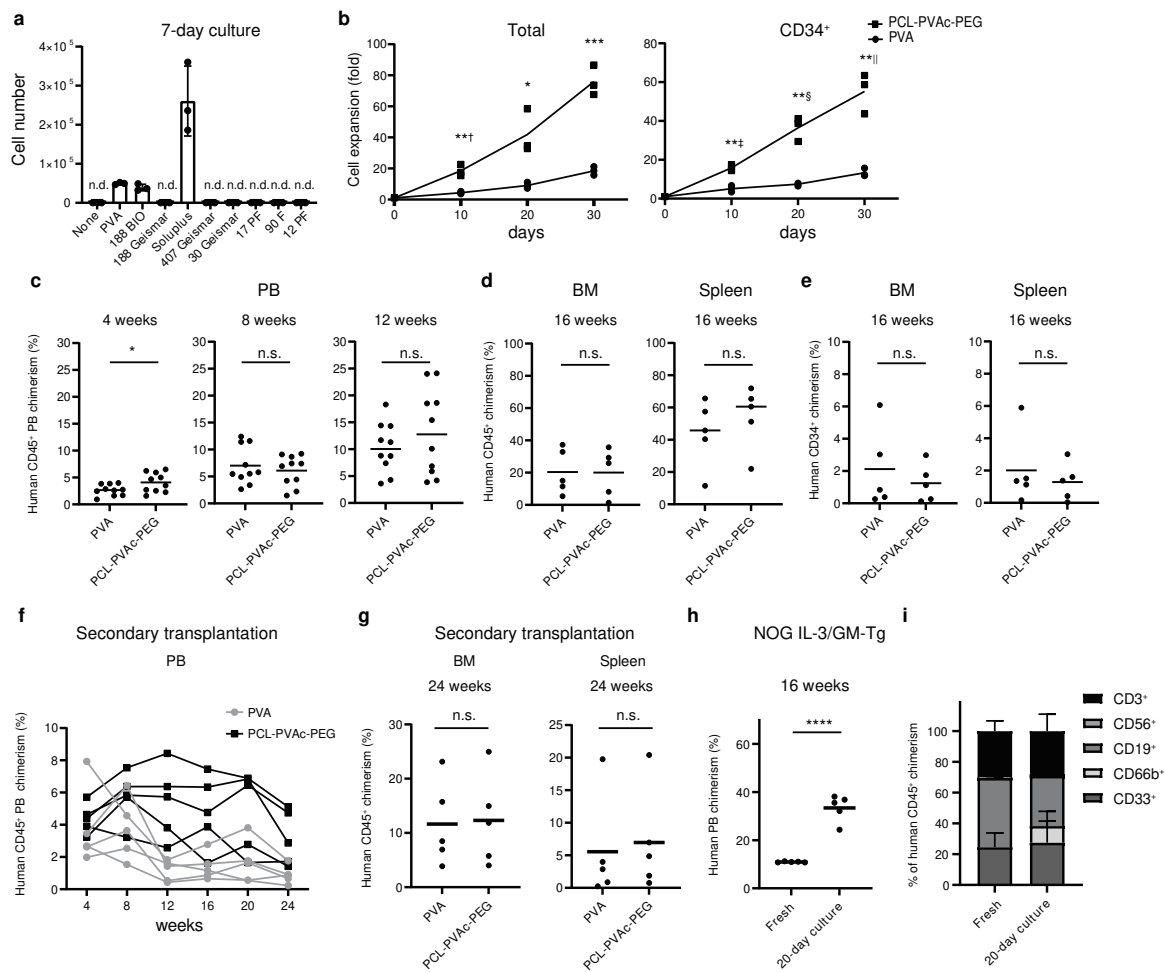
Figure 1 Sakurai, et al.

Figure 2 Sakurai, et al.
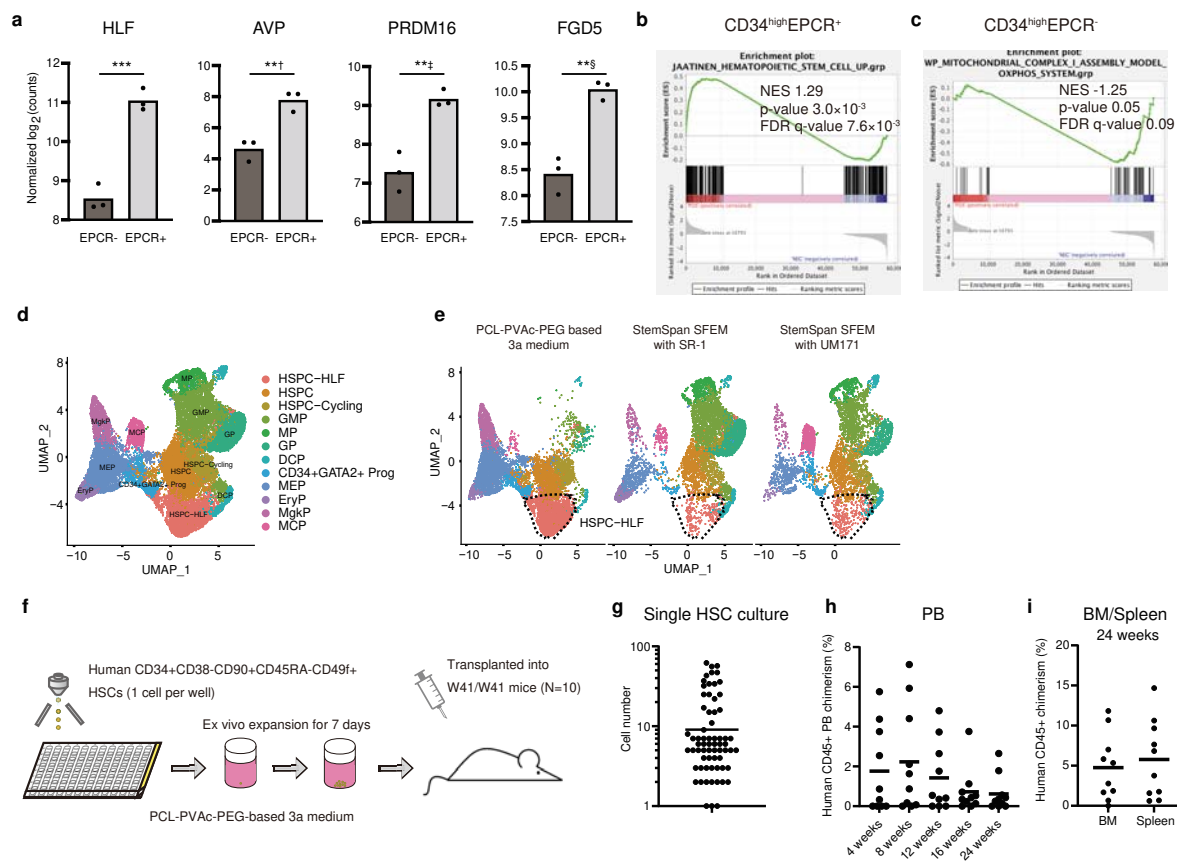
Figure 3 Sakurai, et al.

Figure 4 Sakurai, et al.